© Copyright, Princeton University Press. No part of this book may be distributed, posted, or reproduced in any form by digital or mechanical means without prior written permission of the publisher.

Contents

ition	vii
Edition	xi
POLYGONS	
an Curve Theorem	1
	5
_	9
Gallery Theorem	16
Congruence in 2D	22
Congruence in 3D	28
2 CONVEX HULLS	
	38 38
•	41
	44
e	47
	51
	53
Hull in 3D	56
TONS	65
	65
	72
_	79
	85
riangulations	94
IAGRAMS	107
	107
•	112
	116
	122
9	124
	an Curve Theorem s and Triangulations Combinatorics Gallery Theorem Congruence in 2D Congruence in 3D LLS y tal Construction of Algorithms pping and Graham Scan bund and Conquer Hull in 3D CIONS ms and Combinatorics Graph ciahedron of Triangulations

© Copyright, Princeton University Press. No part of this book may be distributed, posted, or reproduced in any form by digital or mechanical means without prior written permission of the publisher.

vi CONTENTS

5	SHA	SHAPE RECOVERY	
	5.1	Medial Axis	136
	5.2	Straight Skeleton	143
	5.3	Curve Reconstruction	147
	5.4	Disks and Deformations	154
	5.5	The Alpha Complex	158
	5.6	Alpha Complex Construction	162
6	POI	LYGONAL CHAINS	170
	6.1	Cauchy's Arm Lemma	170
	6.2	•	173
	6.3	e e e e e e e e e e e e e e e e e e e	178
	6.4		183
	6.5	Shortening Chains	189
7	7 POLYHEDRA		199
_		Platonic Solids	199
		Euler's Polyhedral Formula	205
	7.3	•	214
		Cauchy's Rigidity Theorem	220
	7.5	. e .	228
	7.6	e e e e e e e e e e e e e e e e e e e	233
	7.7		239
	7.8	8	244
Appen	ıdix: (Computational Complexity	253
Index			259

POLYGONS 1

Polygons are to planar geometry as integers are to numerical mathematics: a discrete subset of the full universe of possibilities that lends itself to efficient computations. And triangulations are the prime factorizations of polygons, alas without the benefit of the *fundamental theorem of arithmetic* guaranteeing unique factorization. This chapter introduces polygons (Section 1.1), triangulations (Section 1.2) and their combinatorics (Section 1.3), applying these concepts to the alluring art gallery theorem (Section 1.4), a topic at the roots of computational geometry that continues to remain an active area of research. Here we encounter a surprising difference between 2D triangulations and 3D tetrahedralizations.

Triangulations are highly constrained decompositions of polygons. Dissections are less constrained partitions, and engender the fascinating question of which pairs of polygons can be dissected and reassembled into one another. This so-called *scissors congruence* (Section 1.5) again highlights the fundamental difference between 2D and 3D (Section 1.6), a theme throughout the book.

1.1 THE JORDAN CURVE THEOREM

Computational geometry is fundamentally *discrete* as opposed to continuous. Computation with curves and smooth surfaces is generally considered part of another field, often called *geometric modeling*. The emphasis on computation leads to a focus on representations of geometric objects that are simple and easily manipulated. Fundamental building blocks are the *point* and the line *segment*, the portion of a line between two points. From these are built more complex structures. Among the most important of these structures are 2D polygons and their 3D generalization, polyhedra.

A $polygon^1$ P is the closed region of the plane bounded by a finite collection of line segments forming a closed curve that does not intersect itself. The line segments are called edges and the points where adjacent edges meet are called vertices. In general, we insist that vertices be true corners at which there is a bend between the adjacent edges, but in some circumstances (such as in Chapter 2) it will be useful to recognize "flat vertices." The set of vertices and edges of P is called the boundary of the polygon,

¹ Often the term *simple polygon* is used, to indicate that it is "simply connected."

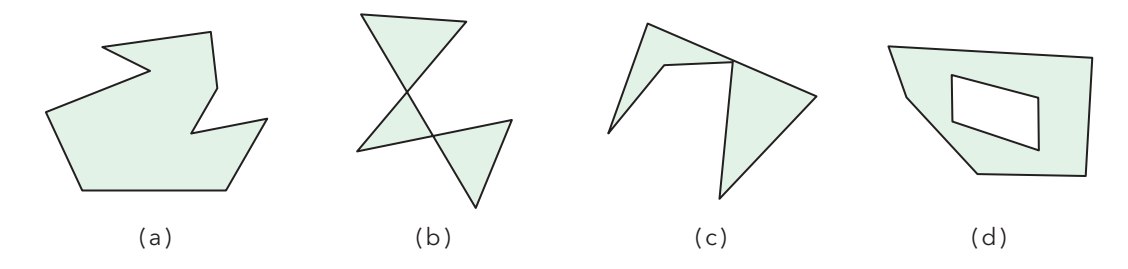


Figure 1.1. (a) Polygon and (b,c,d) objects that are not polygons.

denoted as ∂P . Figure 1.1(a) shows a polygon with nine edges joined at nine vertices. Diagrams (b,c,d) show objects that fail to be polygons.

The fundamental *Jordan curve theorem*, formulated and proved by Camille Jordan in 1882, states that a closed curve on the plane that does not self-intersect divides the plane into two distinct regions, the *interior* and the *exterior* of the curve. This result is notorious for being both obvious and quite difficult to prove in its full generality. But even for polygons, this statement is not obvious. Interior and exterior regions seem straightforward for squares and hexagons, but not necessarily for an example such as the left-hand drawing in Figure 1.2. Our eyes can quickly master this example, but for a polygon with thousands if not millions of edges, visual scanning is unreliable.

There is where the discrete nature of a polygon P, built from a finite collection of vertices and straight edges, comes to the rescue. Begin by choosing a fixed direction in the plane that is not parallel to any edge of P. For any point x on the plane not on ∂P , consider a ray from x in the chosen direction (where a ray is a half-infinite line). Let x belong to

- 1. the *interior* set if the ray intersects ∂P an odd number of times, or 2. the *exterior* set if this ray intersects ∂P an even number of times.
- When the ray passes through a vertex v of ∂P , count it as an intersection only when the two edges incident to v are on different sides of the ray. In

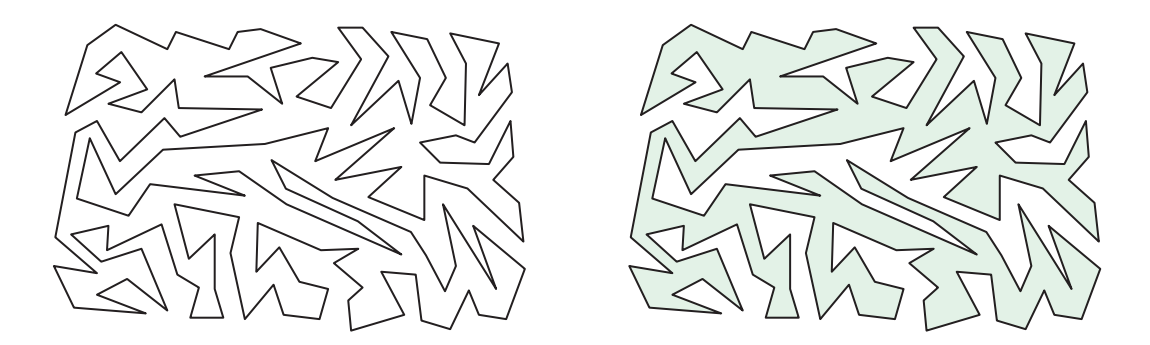


Figure 1.2. A polygonal boundary along with its interior shaded.

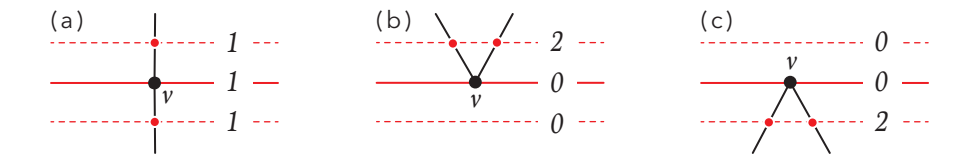


Figure 1.3. Rays passing through vertices.

other words, the (red) ray going through vertex v in Figure 1.3(a) counts, but the rays passing through the vertices in (b) and (c) do not. We count vertices in this manner because small perturbations of the ray preserve parity: If the ray is slightly moved above or below the vertex of intersection (the dashed lines in Figure 1.3), part (a) retains the same intersection count whereas parts (b) and (c) either increase or decrease the count by 2. Regardless, the overall *parity* (odd or even information) of all intersections remains the same, and our two sets (interior and exterior) are well defined.

Exercise 1.1. Show that any two points close enough, but on opposite sides of an edge of ∂P , will have different parity.

Exercise 1.2. If a line segment does not intersect ∂P , show that all of its points must belong to the same parity set.

Exercise 1.3. Let x be a point not on ∂P . Extend the definition of counting intersections to include rays from x parallel to the edges of P. Use this to show that the parity of the intersections-count for any ray from x remains the same.

What remains is to ensure that these sets are properly connected regions, as guaranteed by the following result.

Theorem 1.4 (Polygonal Jordan Curve). The boundary ∂P of a polygon P partitions the plane into two regions: the bounded interior and the unbounded exterior.

Sketch of Proof. For any two points x and y not on ∂P , we need to show there exists a polygonal path (a chain of line segments) from x to y that does not intersect ∂P if and only if x and y have the same parity. First consider the forward direction: Assume there exists a polygonal path between x and y which does not intersect ∂P . Since each line segment of this path has the same parity (Exercise 1.2), so does the entire path, ensuring its endpoints x and y are in the same set.

For the converse direction, assume x and y have the same parity and draw a line segment between them. If this xy segment does not intersect ∂P , then we have found our path. Otherwise, let x' and y' be the first and

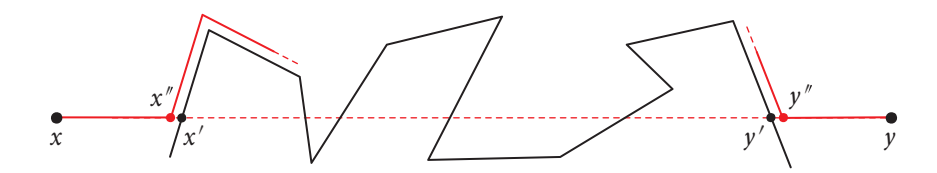


Figure 1.4. Walking close to the edges of the polygon.

last intersections of this segment with ∂P , respectively. Moreover, let x'' be the point obtained by walking from x along xy but stopping just before reaching x', and similarly, let y'' be obtained walking from y, as shown in Figure 1.4. By Exercise 1.2 and our assumption, x, x'', y, y'' all have the same parity. We now construct our path from x to y by starting at x, walking to x'', and traveling very close to but not touching ∂P , until we eventually arrive near point y'. But after this arduous journey, on which side of ∂P at y' does the path arrive: the side containing y'' or the other side? By the forward direction of this proof, since our walk never crossed ∂P , we arrive at a place with the same parity as x. And by Exercise 1.1, we must be on the side of y''. Thus, extending this walk from y'' to y completes the same-parity path and the proof.

Exercise 1.5. The proof finds points x'' and y'' that are "very close" to ∂P . Based on the lengths of the edges of P, provide concrete distances that can bring rigor to this notion of closeness.

Our construction of interior and exterior sets is the basis for an *algorithm*, a blueprint of instructions on how to calculate what the theorem ensures exists. In particular, we can computationally decide whether a given point is in the interior of a polygon, allowing us to verify the shading found on the right of Figure 1.2. This low-level task is encountered every time a user clicks inside some region in a computer game, and in numerous other applications. Throughout this book, our emphasis will be on the geometry that underlies both an algorithm's structure and its proof.

POLYGON INTERIOR ALGORITHM

Point-in-Polygon

Choose a fixed direction in the plane not parallel to any edge of polygon P. Point x is in the interior (exterior) of P if the ray from x in the chosen direction intersects ∂P an odd (even) number of times.

Exercise 1.6. The above algorithm sketch does not address the possibility that x is directly on ∂P . Suggest how to handle this case.

5

1.2 DIAGONALS AND TRIANGULATIONS

Algorithms often need to break polygons into pieces for processing. A natural decomposition of a polygon P into simpler pieces is achieved by drawing diagonals. A diagonal of a polygon is a line segment connecting two vertices of P and lying in the interior of P, not touching ∂P except at its endpoints. Two diagonals are noncrossing if they share no interior points. Figure 1.5(a) shows a diagonal, and (b,c,d) nondiagonals.

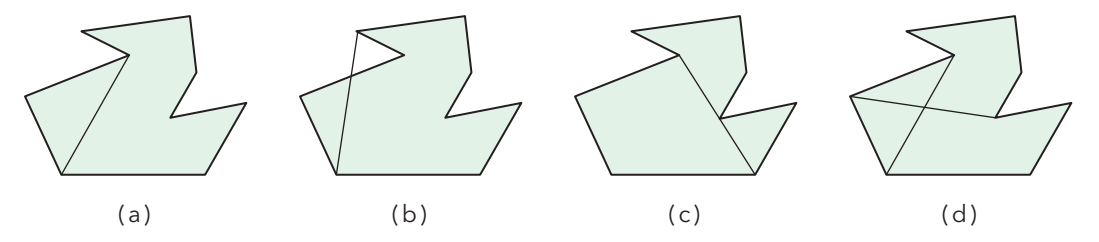


Figure 1.5. (a) A polygon with a diagonal, (b,c) nondiagonal line segments, and (d) nondiagonal crossing segments.

Definition. A triangulation of a polygon P is a decomposition of P into triangles by a maximal set of noncrossing diagonals.

Here, maximal means that no further diagonal may be added to the set without crossing (sharing an interior point with) one already in the set. Figure 1.6 shows a polygon with three different triangulations.

Exercise 1.7. Suppose the partition of P induced by a collection of diagonals D includes a quadrilateral. Argue that D is not maximal.

Triangulations lead to several natural questions: How many triangles are in each triangulation of a given polygon? How many different triangulations does a specific polygon have? Is it true that every polygon has even one triangulation? Does every polygon have at least one diagonal? We start with the last question.

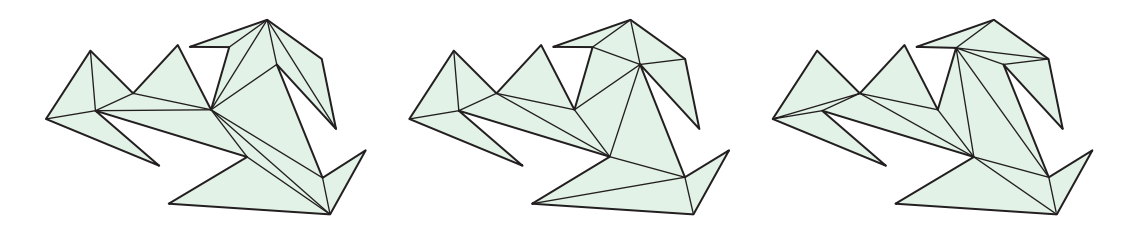


Figure 1.6. A polygon and three possible triangulations.

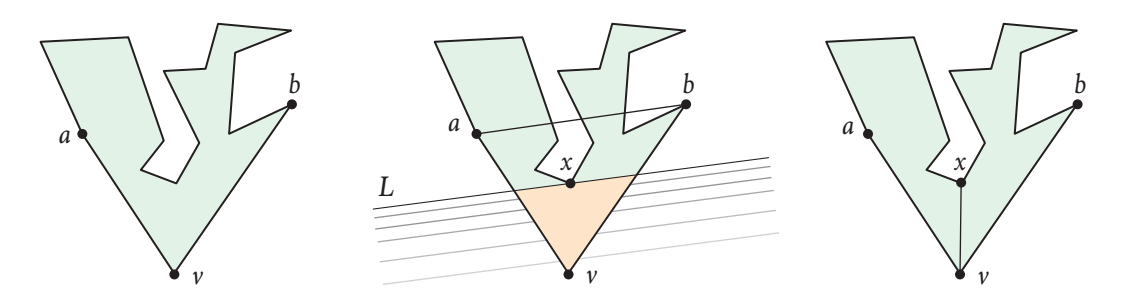


Figure 1.7. Finding a diagonal of a polygon via sweeping.

Lemma 1.8. Every polygon with more than three vertices has a diagonal.

Proof. Let v be the lowest vertex of P; if there are several, let v be the rightmost. Let a and b be the two vertices adjacent to v. If the segment ab lies in P and does not otherwise touch ∂P , it is a diagonal. Otherwise, since P has more than three vertices, the closed triangle formed by a, b, and v contains at least one vertex of P. Let E be a line parallel to segment E passing through E. Sweep this line from E parallel to itself, upward toward E see Figure 1.7. Let E be the first vertex in the closed triangle E different from E by or E that E meets along this sweep. If E meets several vertices simultaneously, let E be the rightmost. The (shaded) triangular region of the polygon below line E and above E is empty of vertices of E. Because E cannot intersect E0 except at E0 and E1, we conclude that E2 is a diagonal.

Since we can decompose any polygon (with more than three vertices) into two smaller polygons using a diagonal, induction leads to the existence of a triangulation.

Theorem 1.9. Every polygon has a triangulation.

Proof. We prove this by induction on the number of vertices n of the polygon P. If n = 3, then P is a triangle and we are finished. Let n > 3 and assume the theorem is true for all polygons with fewer than n vertices. Using Lemma 1.8, find a diagonal cutting P into polygons P_1 and P_2 . Because both P_1 and P_2 have fewer vertices than n, P_1 and P_2 can be triangulated by the induction hypothesis. By the polygonal Jordan curve theorem (Theorem 1.4), the interior of P_1 is in the exterior of P_2 , and so no triangle of P_1 will share an interior point with a triangle of P_2 . A similar statement holds for the triangles of P_2 . Thus P has a triangulation as well.

Exercise 1.10. Prove that every polygonal region with polygonal holes, such as Figure 1.1(d), admits a triangulation of its interior.

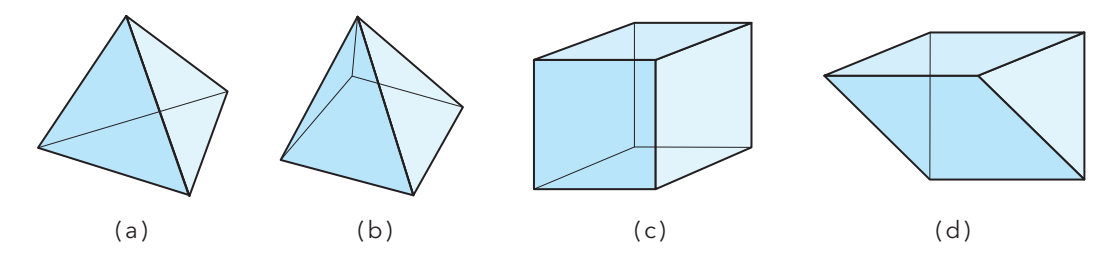


Figure 1.8. Polyhedra examples: (a) tetrahedron, (b) pyramid with square base, (c) cube, and (d) triangular prism.

That every polygon has a triangulation is a fundamental property that pervades discrete geometry and will be used over and over again in this book. It is remarkable that this notion does not generalize smoothly to three dimensions. A *polyhedron* is the 3D version of a polygon, a 3D solid bounded by finitely many polygons; Figure 1.8 shows some examples. Chapter 7 will define polyhedra more precisely and explore them more thoroughly. Here we rely on intuition.

Just as the simplest polygon is the triangle, the simplest polyhedron is the *tetrahedron*: a pyramid with a triangular base. We can generalize the 2D notion of polygon triangulation to 3D: A *tetrahedralization* of a polyhedron is a partition of its interior into tetrahedra whose six edges are either polyhedron edges or diagonals of the polyhedron. Figure 1.9 shows examples of tetrahedralizations of the polyhedra just illustrated.

Exercise 1.11. *Find a tetrahedralization of the cube into five tetrahedra.*

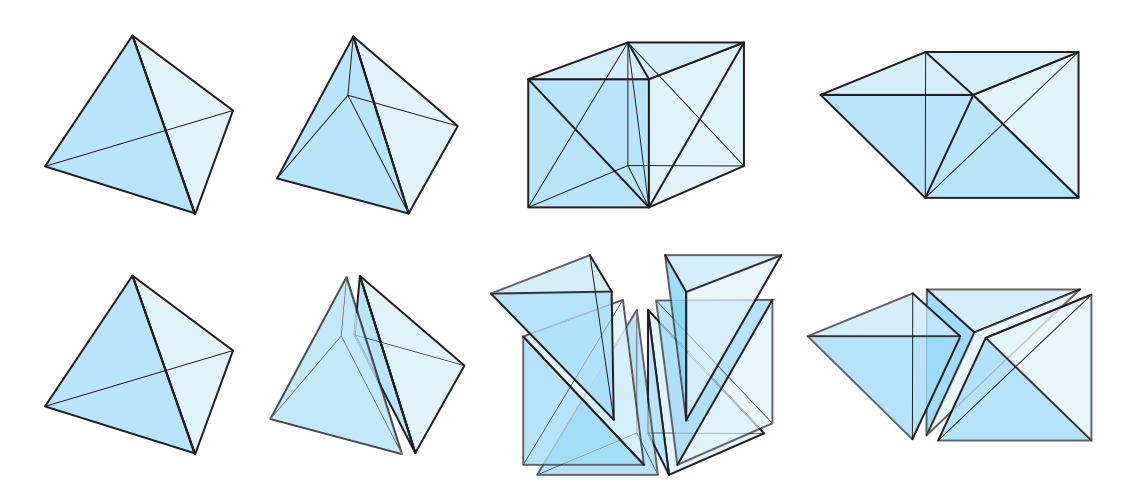


Figure 1.9. Tetrahedralizations of the polyhedra from Figure 1.8.

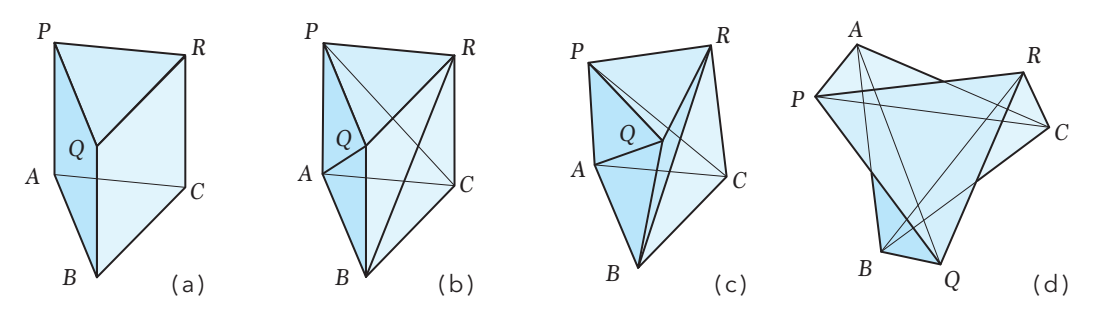


Figure 1.10. Construction of the Schönhardt polyhedron from a triangular prism, where (d) is the overhead view.

We proved in Theorem 1.9 that all polygons can be triangulated. Does the analogous claim hold for polyhedra? That is, can all polyhedra be tetrahedralized? In 1911, Nels Lennes proved the surprising theorem that this is not so. We construct an example of a polyhedron, based on the 1928 model by Erich Schönhardt, which cannot be tetrahedralized. Let A, B, C be vertices of an equilateral triangle (labeled counterclockwise) in the xy-plane. Extruding this triangle vertically along the z-axis reaching z=1 traces out a triangular prism, as shown in Figure 1.10(a). Part (b) shows the prism with the faces partitioned by the diagonal edges AQ, BR, and CP. Now twist the top PQR triangle $\pi/6$ radians in the (z=1)-plane, rotating and stretching the diagonal edges. The result is the Schönhardt polyhedron, shown in (c) and in an overhead view in (d) of the figure. Schönhardt proved that this is the smallest example of an untetrahedralizable polyhedron.

Exercise 1.12. Prove that the Schönhardt polyhedron cannot be tetrahedralized.

UNSOLVED PROBLEM 1

Tetrahedralizable Polyhedra

Find characteristics that determine whether or not a polyhedron is tetrahedralizable. Even identifying a large natural class of tetrahedralizable nonconvex polyhedra would be interesting.

This is indeed a difficult problem. It was proved by Jim Ruppert and Raimund Seidel in 1992 that it is *NP-complete* to determine whether a polyhedron is tetrahedralizable. "NP-complete" is a technical term from complexity theory that means, roughly, an intractable algorithmic problem. (See the Appendix for a more thorough explanation.) It suggests in this case that there is almost certainly no succinct characterization of tetrahedralizability.

1.3 POLYGON COMBINATORICS

We know that every polygon has at least one triangulation. Next we show that the number of triangles in any triangulation of a fixed polygon is the same. The proof is essentially the same as that of Theorem 1.9, with more quantitative detail.

Theorem 1.13. Every triangulation of a polygon P with n vertices has n-2 triangles and n-3 diagonals.

Proof. We prove this by induction on n. When n=3, the statement is trivially true. Let n>3 and assume the statement is true for all polygons with fewer than n vertices. Choose a diagonal d joining vertices a and b, cutting P into polygons P_1 and P_2 having n_1 and n_2 vertices, respectively. Because a and b appear in both P_1 and P_2 , we know $n_1 + n_2 = n + 2$. The induction hypothesis implies that there are $n_1 - 2$ and $n_2 - 2$ triangles in P_1 and P_2 , respectively. Hence P has

$$(n_1-2) + (n_2-2) = (n_1+n_2) - 4 = (n+2) - 4 = n-2$$

triangles. Similarly, P has $(n_1 - 3) + (n_2 - 3) + 1 = n - 3$ diagonals, with the +1 term counting d.

Many proofs and algorithms that involve triangulations need a special place to initiate induction or start recursion. "Ears" often serve this role. Three consecutive vertices a, b, c form an ear of a polygon if ac is a diagonal of the polygon. The vertex b is called the ear tip.

Corollary 1.14. Every polygon with more than three vertices has at least two ears with nonadjacent tips.

Proof. Consider any triangulation of a polygon P with n > 3 vertices, which by Theorem 1.13 partitions P into n-2 triangles. Each triangle covers at most two edges of ∂P . Because there are n edges on the boundary of P but only n-2 triangles, by the pigeonhole principle at least two triangles must contain two edges of P. These are the ears.

Exercise 1.15. Prove Corollary 1.14 using induction.

Exercise 1.16. Show that the sum of the interior angles of any polygon with n vertices is $\pi(n-2)$.

Exercise 1.17. Using the previous exercise, show that the total turn angle around the boundary of a polygon is 2π . Here the turn angle at a vertex v is π minus the internal angle at v.

Exercise 1.18. Three consecutive vertices a, b, c form a mouth of a polygon if ac is an external diagonal of the polygon, a segment wholly outside. Formulate and prove a theorem about the existence of mouths.

Exercise 1.19. Let a polygon P with h holes have n total vertices (including hole vertices). Find a formula for the number of triangles in any triangulation of P as a function of n and h.

Exercise 1.20. Let P be a polygon with vertices (x_i, y_i) in the plane. Prove that the area of P is

 $\frac{1}{2} \left| \sum (x_i y_{i-1} - x_{i-1} y_i) \right|.$

Although the number of triangles in any triangulation of a polygon is the same, it is natural to explore the number of different triangulations of a given polygon. For instance, Figure 1.6 shows a polygon with three different triangulations.

Exercise 1.21. For each polygon in Figure 1.11, find the number of distinct triangulations.

Exercise 1.22. For each n > 3, find a polygon with n vertices that has a unique triangulation.

The number of triangulations of a fixed polygon P has much to do with the "shape" of the polygon. One crucial measure of shape is the internal angles at the vertices. A vertex of P is called *reflex* if its angle is greater than π , and *convex* if its angle is less than or equal to π . As mentioned in Section 1.1, sometimes it is useful to distinguish a *flat* vertex, whose angle is exactly π , from a *strictly convex* vertex, whose angle is strictly less than π . A polygon P is a *convex* polygon if all vertices of P are convex. In general we exclude flat vertices, so unless otherwise indicated, the vertices of a convex polygon are strictly convex. With this understanding, a convex polygon has the following special property.

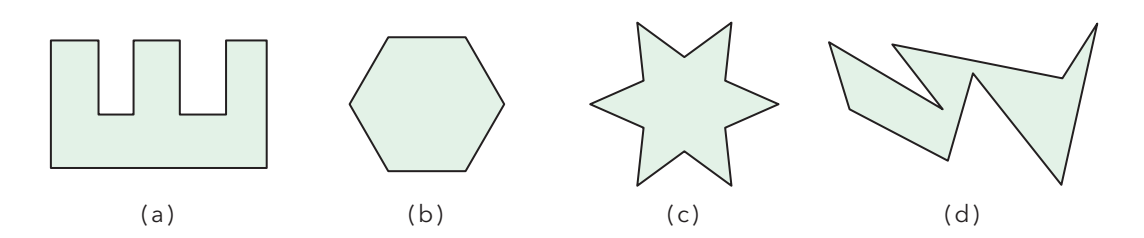


Figure 1.11. How many distinct triangulations for these polygons?

Lemma 1.23. A diagonal exists between any two nonadjacent vertices of a polygon P if and only if P is a convex polygon.

Proof. The proof is in two parts, both established by contradiction. First assume *P* is not convex. We need to find two vertices of *P* that do not form a diagonal. Because *P* is not convex, there exists a sequence of three vertices *a*, *b*, *c*, with *b* reflex. Then the segment *ac* lies (at least partially) exterior to *P* and so is not a diagonal.

Now assume P is convex but there is a pair of vertices a and b in P that do not form a diagonal. We identify a reflex vertex of P to establish the contradiction. Let σ be the shortest path connecting a to b entirely within P. It cannot be that σ is a straight segment contained inside P, for then ab is a diagonal. Instead, σ must be a chain of line segments. Each corner of this polygonal chain turns at a reflex vertex—if it turned at a convex vertex or at a point interior to P, it would not be the shortest.

Exercise 1.24. For any two points x and y in a polygon P, prove that the line segment xy lies in P if and only if P is convex.

For a convex polygon *P*, where every pair of nonadjacent vertices determines a diagonal, it is possible to count the number of triangulations of *P* based solely on the number of vertices. The result is the *Catalan number*, named after the 19th-century Belgian mathematician Eugène Catalan, which uses the binomial coefficient

$$\binom{n}{k} \coloneqq \frac{n!}{k!(n-k)!}$$

that counts the different combinations of choosing n distinct objects taken k at a time, where choosing order does not matter.

Theorem 1.25. The number of triangulations of a convex polygon with n+2 vertices is the Catalan number

$$C_n = \frac{1}{n+1} \binom{2n}{n}. (1.1)$$

Proof. Let P_{n+2} be a convex polygon with n+2 vertices labeled from 1 to n+2 counterclockwise. Let \mathcal{T}_{n+2} be the set of triangulations of P_{n+2} , where \mathcal{T}_{n+2} has t_{n+2} elements. We wish to show that t_{n+2} is the Catalan number C_n .

We proceed by induction on the number of vertices. For the base case triangle P_3 , notice that $t_3 = 1 = C_1$, as desired. Assume the result $t_{i+2} = C_i$ holds for all convex polygons up to n+1 vertices. Now consider a polygon P_{n+2} with n+2 vertices. Contract the edge $\{1, n+2\}$

of P_{n+2} and let ϕ be the map from set \mathcal{T}_{n+2} to set \mathcal{T}_{n+1} given by this contraction.²

For T an element of \mathcal{T}_{n+1} , what is important to note is the number of triangulations of \mathcal{T}_{n+2} that contract to T (i.e., the number of elements of $\phi^{-1}(T)$) equals the degree of vertex 1 in T. Figure 1.12 shows an example where (a) five triangulations of the octagon all contract to (b) the same triangulation T of the heptagon, where the vertex labeled 1 has degree five in T. This is evident since each edge incident to 1 can expand into a triangle in $\phi^{-1}(T)$, shown by the shaded triangles in (a). So we see that

$$t_{n+2} = \sum_{T \in \mathcal{T}_{n+1}}$$
 degree of vertex 1 of T .

Because this polygon is convex, this is true for all vertices of T. Therefore we can sum over all of these n+1 vertices, obtaining

$$(n+1) \cdot t_{n+2} = \sum_{i=1}^{n+1} \sum_{T \in \mathcal{T}_{n+1}} \text{degree of vertex } i \text{ of } T$$
$$= \sum_{T \in \mathcal{T}_{n+1}} \sum_{i=1}^{n+1} \text{degree of vertex } i \text{ of } T.$$

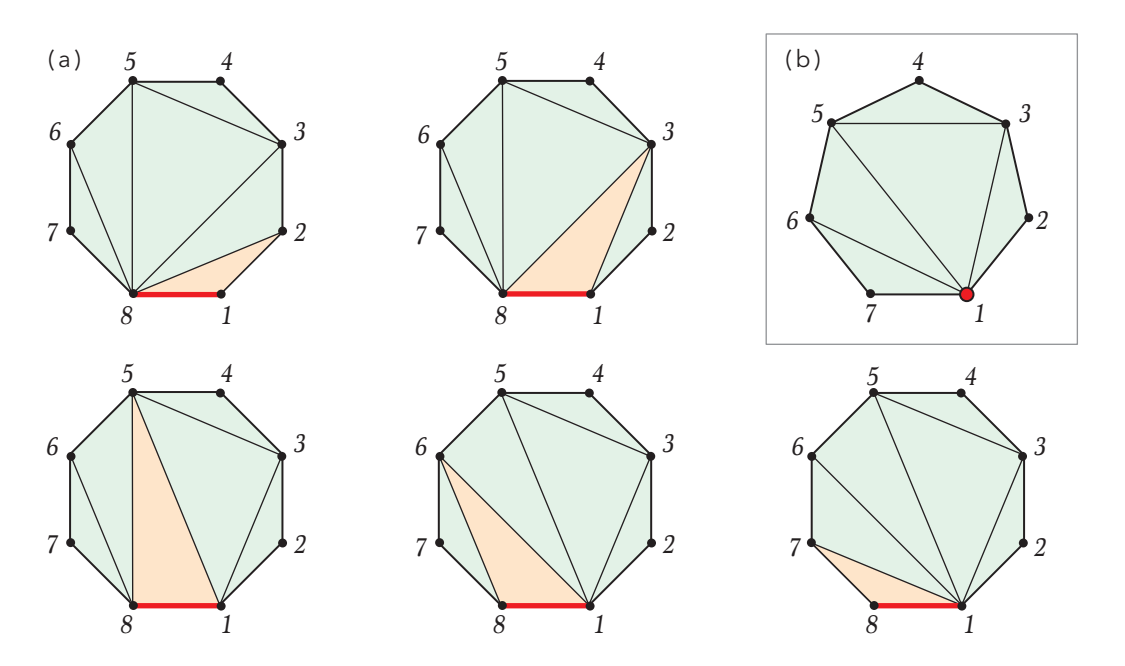


Figure 1.12. The five polygons in (a) all map to the same polygon T in (b) under contraction of edge $\{1, 8\}$.

² To *contract* an edge ab is to shrink it to a point c so that c becomes incident to all the edges and diagonals that were incident to either a or b.

The right-hand side of this equation asks for the sum of the degrees of all vertices of T, for each triangulation T in \mathcal{T}_{n+1} . But this sum double counts both the number of edges and the number of diagonals of T. Since T has n+1 edges and n-2 diagonals (by Theorem 1.13), we have

$$(n+1) \cdot t_{n+2} = \sum_{T \in \mathcal{T}_{n+1}} 2((n+1) + (n-2)) = 2(2n-1) \cdot t_{n+1}.$$

Solving for t_{n+2} yields

$$t_{n+2} = \frac{2(2n-1)}{n+1} \cdot t_{n+1}.$$

By the induction hypothesis, this becomes

$$t_{n+2} = \frac{2(2n-1)}{n+1} \cdot C_{n-1} = \frac{2(2n-1)}{n+1} \cdot \frac{1}{n} {2n-2 \choose n-1} = C_n,$$

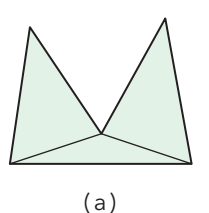
completing the proof.

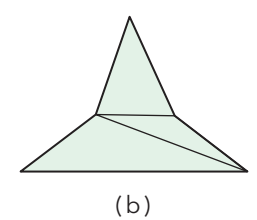
For the octagon in Figure 1.12, the formula shows there are $C_6 = 132$ distinct triangulations. Is it possible to find a closed formula for the number of triangulations for nonconvex polygons P with n vertices? The answer, unfortunately, is no, because small changes in the positions of vertices can lead to vastly different triangulations of the polygon. What we do know is that convex polygons achieve the maximum number of triangulations.

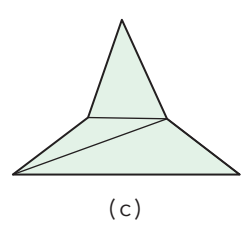
Theorem 1.26. Let P be a polygon with n+2 vertices. The number of triangulations of P is between 1 and C_n .

Proof. Exercise 1.22 shows there are polygons with exactly one triangulation, demonstrating that the lower bound is realizable. For the upper bound, let P be any polygon with n + 2 labeled, ordered vertices, and let Q be a convex polygon also with n + 2 vertices, labeled similarly. Each diagonal of P corresponds to a similarly labeled diagonal of Q, and if two diagonals do not cross in P, neither do they cross in Q. So every triangulation of P (having n - 1 diagonals by Theorem 1.13) determines a triangulation of Q (again with n - 1 diagonals). Therefore, P can have no more triangulations than Q, which by Theorem 1.25 is C_n .

Thus we see that convex polygons yield the most triangulations. Because convex polygons have no reflex vertices (by definition), there might possibly be a relationship between the number of triangulations and the number of reflex vertices of a polygon. Sadly, this is not the case. Let *P* be a polygon with five vertices. By Theorem 1.25, if *P* has no reflex vertices, it must have five triangulations. Figure 1.13(a) shows *P* with one reflex vertex and only one triangulation, whereas parts (b) and (c) show *P* with two reflex vertices and two triangulations. So the number of triangulations does not







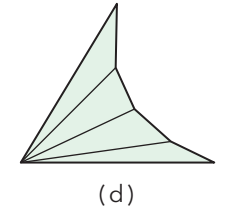


Figure 1.13. Triangulations of polygons with reflex vertices.

necessarily decrease with the number of reflex vertices. In fact, the number of triangulations does not depend on the number of reflex vertices at all. Figure 1.13(d) shows a polygon with a unique triangulation with three reflex vertices. This example can be generalized to polygons with unique triangulations that contain arbitrarily many reflex vertices.

Exercise 1.27. For each n > 3, find a polygon with n vertices with exactly two triangulations.

Exercise 1.28. For any $n \ge 3$, show there is no polygon with n + 2 vertices with exactly $C_n - 1$ triangulations.

UNSOLVED PROBLEM 2

Counting Triangulations

Identify features of polygons *P* that lead to a closed formula for the number of triangulations of *P* in terms of those features.

We learned earlier that properties can be lost in the move from 2D polygons to 3D polyhedra. As we saw, all polygons can be triangulated but not all polyhedra can be tetrahedralized. Moreover, by Theorem 1.13 above, we know that *every* polygon with *n* vertices must have the same number of triangles in *any* of its triangulations. For polyhedra, this is far from true. In fact, two different tetrahedralizations of the *same* polyhedron can result in a different number of tetrahedra! Consider Figure 1.14, which shows a polyhedron partitioned into (a) two tetrahedra and also into (b) three tetrahedra.

Even for a polyhedron as simple as the cube, the number of tetrahedra is not the same for all tetrahedralizations. It turns out that, up to rotation and reflection, there are six different tetrahedralizations of the cube, one of which was shown earlier in Figure 1.9. Five of the six partition the cube into six tetrahedra, but one cuts it into only five tetrahedra (see Exercise 1.11).

Exercise 1.29. Is it possible to partition a cube into six congruent tetrahedra? Defend your answer.

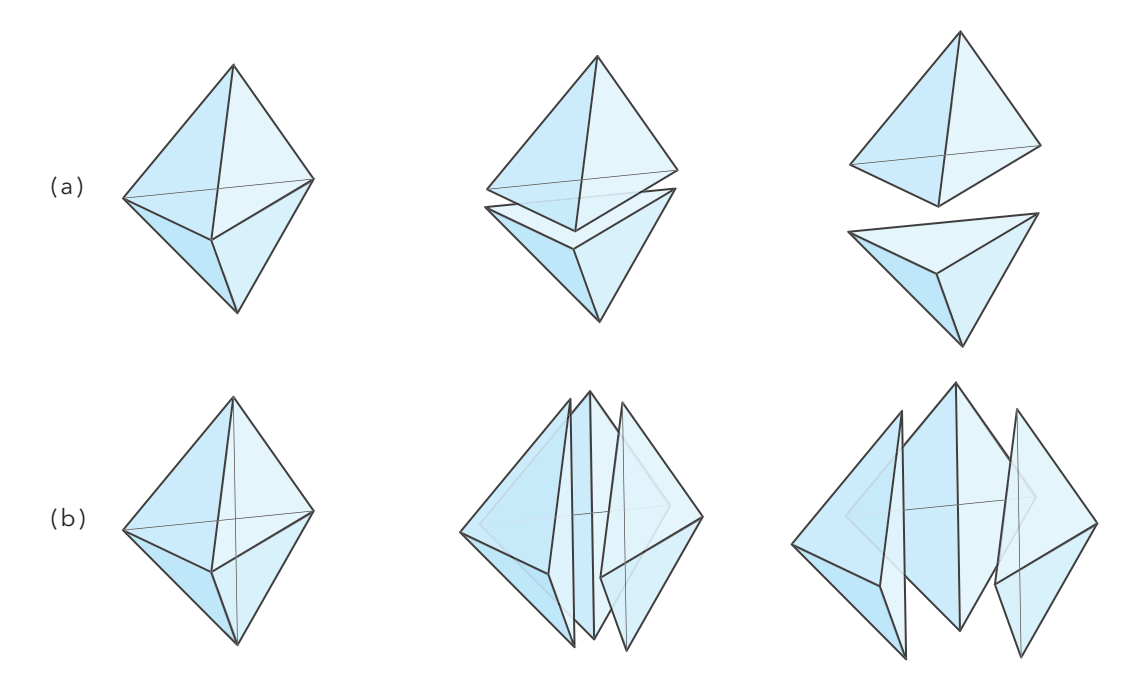


Figure 1.14. A polyhedron partitioned into (a) two and (b) three tetrahedra.

Exercise 1.30. Find the six different tetrahedralizations of the cube up to rotation and reflection.

Exercise 1.31. Classify the set of triangulations of the boundary of the cube that "induce" tetrahedralizations of the cube, where each such tetrahedralization matches the triangulation on the cube surface.

Just as the tetrahedron is the 3D version of the 2D triangle, the *n-simplex* is its *n-*dimensional generalization. Similarly, the *n-cube* is the *n-*dimensional analog of the 2D square and the 3D cube.

Exercise 1.32. *Provide clear definitions of the n-simplex and the n-cube.*

Exercise 1.33. Show that the n-cube can be triangulated into exactly n! n-simplices.

UNSOLVED PROBLEM 3 Minimum Triangulations of Cubes

Find the smallest triangulation of the *n*-cube into *n*-simplices. It is known, for example, that the 4-cube (also known as the *tesseract*) may be partitioned into sixteen 4-simplices, and this is minimal. But the minimum number is unknown except for the few small values of *n* that have yielded to exhaustive computer searches using linear programming.

1.4 THE ART GALLERY THEOREM

A beautiful problem posed by Victor Klee in 1973 engages several of the concepts we have discussed. Imagine an art gallery whose floor plan is modeled by a polygon. A guard in the gallery corresponds to a point on our polygonal floor plan. Guards are posted at fixed locations and can see in every direction, with a full 360° range of visibility. Klee asked: What is the fewest number of guards needed to protect the gallery? Before tackling this problem, we need to define what it means to "see something" mathematically.

A point y in polygon P is *visible* to point x in P if the line segment xy lies in P. This definition allows the line of sight to have a grazing contact with the boundary ∂P (unlike the definition for diagonal—see the earlier Figure 1.5(c)). So xy is nowhere exterior to P. A set of guards *covers* a polygon if every point in the polygon is visible to some guard. Figure 1.15 shows three examples of the range of visibility available to single guards in a polygon.

A natural question is to ask for the *minimum* number of guards needed to cover polygons. Of course, this minimum number depends on the "complexity" of the polygon in some way. We choose to measure complexity in terms of the number of vertices of the polygon. But two polygons with n vertices can require different numbers of guards to cover them. Thus we look for a bound that holds for *any* polygon with n vertices.³

Exercise 1.34. For each polygon in Figure 1.11, find the minimum number of guards needed to cover it.

Exercise 1.35. Suppose that guards themselves block visibility so that a line of sight from one guard cannot pass through the position of another. Are there polygons for which the minimum number of our more powerful guards needed is strictly less than the minimum needed for these weaker guards?

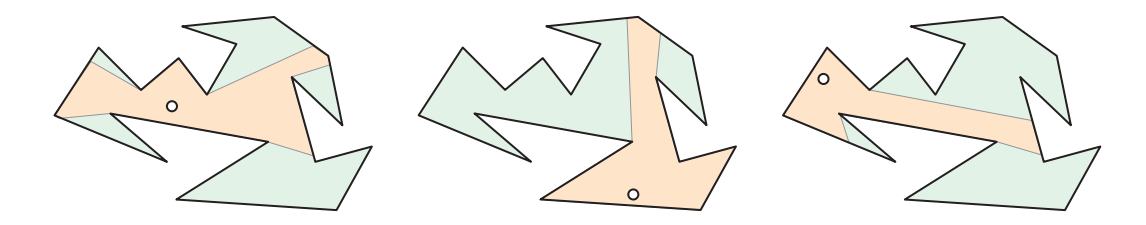


Figure 1.15. Examples of the range of visibility available to certain placements of guards.

³ To find the minimum number of guards for a *particular* polygon turns out to be, in general, an intractable algorithmic task. This is another instance of an NP-complete problem; see the Appendix.

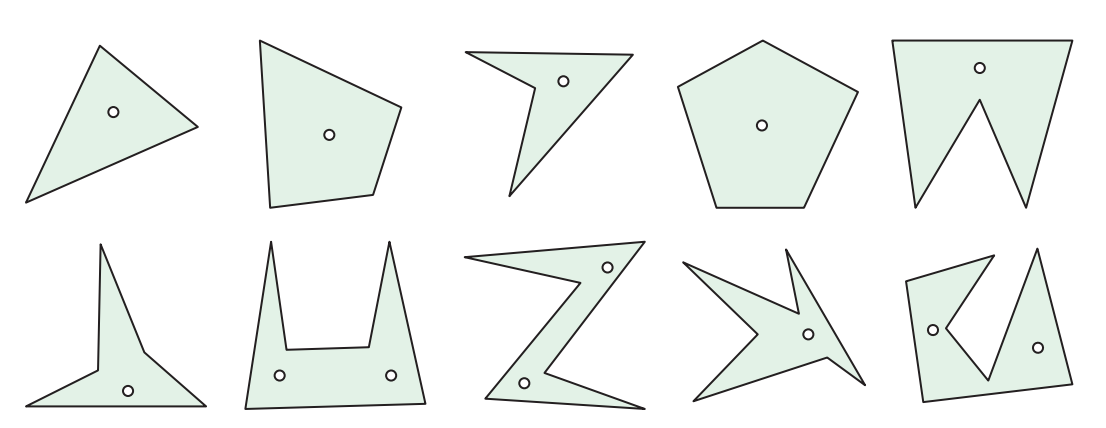


Figure 1.16. Examples of covering guard placements for different polygons.

Let's start by looking at some examples for small values of *n*. Figure 1.16 shows examples of covering guard placements for polygons with a small number of vertices. Clearly, any triangle only needs one guard to cover it. A little experimentation shows that the first time two guards are needed is for certain kinds of hexagons.

Exercise 1.36. Prove that any quadrilateral needs only one guard to cover it. Then prove that any pentagon needs only one guard to cover it.

By Exercise 1.24, convex polygons need only one guard for coverage. The converse of this statement is not true, however. There are polygons that need only one guard but which are not convex. These polygons are called *star-shaped* polygons, or just *star* polygons. The set of points that can see the entire polygon *P* is called the *kernel* of *P*. A guard anywhere in the kernel then covers *P*. Star polygons are the only ones with a nonempty kernel. Figures 1.11(c) and 1.13 show examples.

While correct placement avoids the need for a second guard for quadrilaterals and pentagons, one can begin to see how reflex vertices will cause problems in polygons with large numbers of vertices. Because there can exist only so many reflex angles in a polygon, we can construct a useful example, based on prongs or tines. Figure 1.17 illustrates the comb-shaped design made of 5 prongs and 15 vertices. We can see that a comb of n prongs has 3n vertices, and since each prong needs its own guard, then at least $\lfloor n/3 \rfloor$ guards are needed. Here, the symbols $\lfloor \rfloor$ indicate the floor function: the largest integer less than or equal to the enclosed argument. Thus we have a lower bound on Klee's problem: $\lfloor n/3 \rfloor$ guards are sometimes necessary.

Exercise 1.37. Construct a polygon P and a placement of guards such that the guards see every point of ∂P but not all interior points of P are covered.

⁴ Later we will use its cousin, the *ceiling* function $\lceil \rceil$, the smallest integer greater than or equal to the argument.

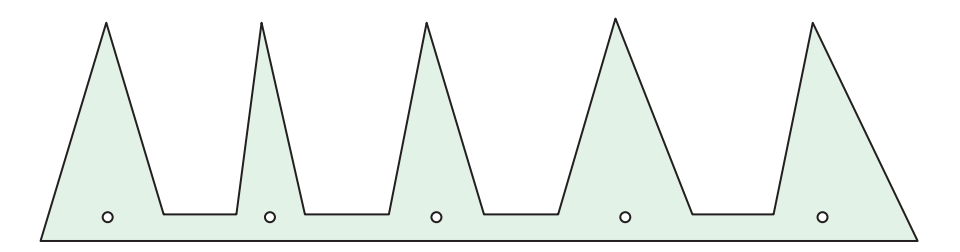


Figure 1.17. A comb-shaped example.

UNSOLVED PROBLEM 4

Visibility Graphs

The *visibility graph* of a polygon *P* is the graph with a node for each vertex of *P* and an arc connecting two nodes when the corresponding vertices of *P* can see one another. Find necessary and sufficient conditions that determine when a graph is the visibility graph of some polygon.

Now that we have a lower bound of $\lfloor n/3 \rfloor$, the next question is whether this number always suffices, that is, whether it is also an upper bound for all polygons. Other than proceeding case by case, how can we attack the problem from a general framework? The answer lies in triangulating the polygon. Theorem 1.9 implies that every polygon with n vertices can be covered with n-2 guards by placing a guard in each triangle, providing a crude upper bound. But we have been able to do better than this already for quadrilaterals and pentagons. By placing guards not in each triangle but at the vertices, we can possibly cover more triangles by fewer guards. In 1975, Vašek Chvátal found a proof for the minimum number of guards needed to cover any polygon with n vertices. His proof is based on induction, with some delicate case analysis. A few years later, Steve Fisk found a beautiful inductive proof, which follows below.

Theorem 1.38 (Art Gallery). To cover a polygon with n vertices, $\lfloor n/3 \rfloor$ vertex guards are needed for some polygons, and are sufficient for all polygons.

Proof. We have already seen in Figure 1.17 that $\lfloor n/3 \rfloor$ guards are sometimes necessary. We now need to show this number also suffices. Consider a triangulation of a polygon P. We use induction to prove that each vertex of P can be assigned one of three colors so that any pair of vertices connected by an edge of P or a diagonal of the triangulation must have different colors. Such a triangulation is said to be 3-colored.

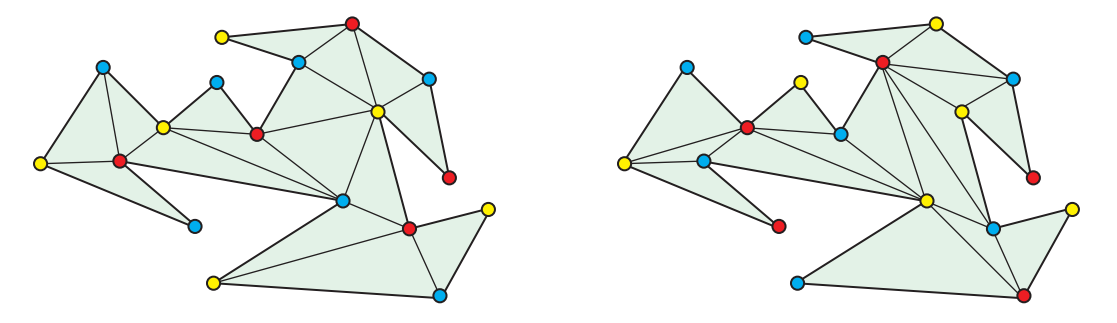


Figure 1.18. Triangulations and colorings of vertices of a polygon with n=18 vertices. In both figures, red is the least frequently used color, occurring five times.

Figure 1.18 shows two examples of triangulations of a polygon along with colorings of the vertices as described.

A triangle is certainly 3-colored. For n > 3, Corollary 1.14 guarantees that P has an ear abc, with vertex b as the ear tip. Deleting this tip produces a polygon P' with n-1 vertices. By the induction hypothesis, the vertices of P' can be 3-colored. Replacing the tip b, and coloring it with the color not used by a or c, provides a 3-coloring for P.

Since there are n vertices, by the pigeonhole principle, the least frequently used color appears on at most $\lfloor n/3 \rfloor$ vertices. Place guards at these vertices. Because every triangle has a vertex of this color, and this guard covers the triangle, the polygon is completely covered.

Exercise 1.39. For each polygon in Figure 1.19, find a minimal set of guards that cover it.

Exercise 1.40. Construct a polygon with n = 3k vertices such that placing a guard at every third vertex counterclockwise fails to protect the gallery.

The classical art gallery problem as presented has been generalized in several directions. Some of these generalizations have elegant solutions, some have difficult solutions, and several remain unsolved problems. For

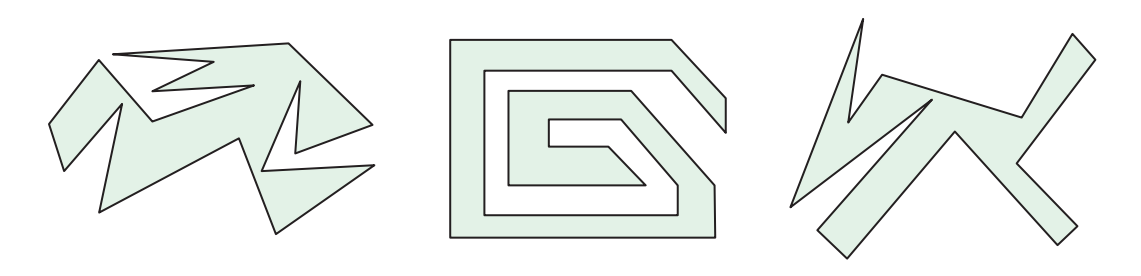


Figure 1.19. Find a set of minimal guards that cover the polygons.

instance, the shape of the polygons can be restricted (to polygons with right-angled corners) or enlarged (to include polygons with holes), or the mobility of the guards can be altered (permitting guards to walk along edges, or along diagonals).

Exercise 1.41. Why is it not possible to easily extend Fisk's proof above to the case of polygons with holes?

Exercise 1.42. Using Exercise 1.19, derive an upper bound on the number of guards needed to cover a polygon with h holes and n total vertices. (Obtaining a tight upper bound is extremely difficult, and only recently settled.)

When all edges of the polygon meet at right angles (an *orthogonal* polygon), fewer guards are needed, as established by Jeff Kahn, Maria Klawe, and Daniel Kleitman in 1980. In contrast, covering the exterior rather than the interior of a polygon requires (in general) more guards.

Theorem 1.43 (Orthogonal Gallery). To cover polygons with n vertices with only right-angled corners, $\lfloor n/4 \rfloor$ guards are needed for some polygons, and sufficient for all polygons.

Theorem 1.44 (Fortress). To cover the exterior of polygons with n vertices, $\lceil n/2 \rceil$ boundary guards are needed for some polygons, and are sufficient for all polygons.

Exercise 1.45. Prove the fortress theorem.

Exercise 1.46. For any n > 3, construct a polygon P with n vertices such that $\lceil n/3 \rceil$ guards, placed anywhere on the plane, are sometimes necessary to cover the exterior of P.

UNSOLVED PROBLEM 5

Edge Guards

An *edge guard* along edge e of polygon P sees a point y in P if there exists x in e such that x is visible to y. Find the number of edge guards that suffice to cover a polygon with n vertices. Equivalently, how many edges, lit as fluorescent light bulbs, suffice to illuminate the polygon? Godfried Toussaint conjectured that $\lfloor n/4 \rfloor$ edge guards suffice, except for a few small values of n.

The art gallery theorem shows that placing a guard at every vertex of the polygon is three times more than needed to cover it. But what about for a polyhedron in three dimensions? It seems almost obvious that guards at every vertex of any polyhedron should cover the interior of the polyhedron. It is remarkable that this is not so.

The reason the art gallery theorem succeeds in two dimensions is the fundamental property that all polygons can be triangulated. Indeed, Theorem 1.9 is not available to us in three dimensions: Not all polyhedra are tetrahedralizable, as demonstrated earlier in Figure 1.10(c). If our polyhedron indeed was tetrahedralizable, then every tetrahedron would have guards in the corners, and all the tetrahedra would then cover the interior.

Exercise 1.47. Let P be a polyhedron with a tetrahedralization where all edges and diagonals of the tetrahedralization lie on the boundary of P. Make a conjecture about the number of guards needed to cover P.

Exercise 1.48. Show that even though the Schönhardt polyhedron (Figure 1.10) is not tetrahedralizable, it is still covered by guards at every vertex.

Because not all polyhedra are tetrahedralizable, the "obviousness" of coverage by guards at vertices is less clear. In 1992, Raimund Seidel, and William Thurston independently, constructed a polyhedron such that guards placed at every vertex do not cover the interior. Figure 1.20 illustrates a version of the polyhedron, which can be constructed as follows. Start with a large cube and let ε be a very small positive number. On

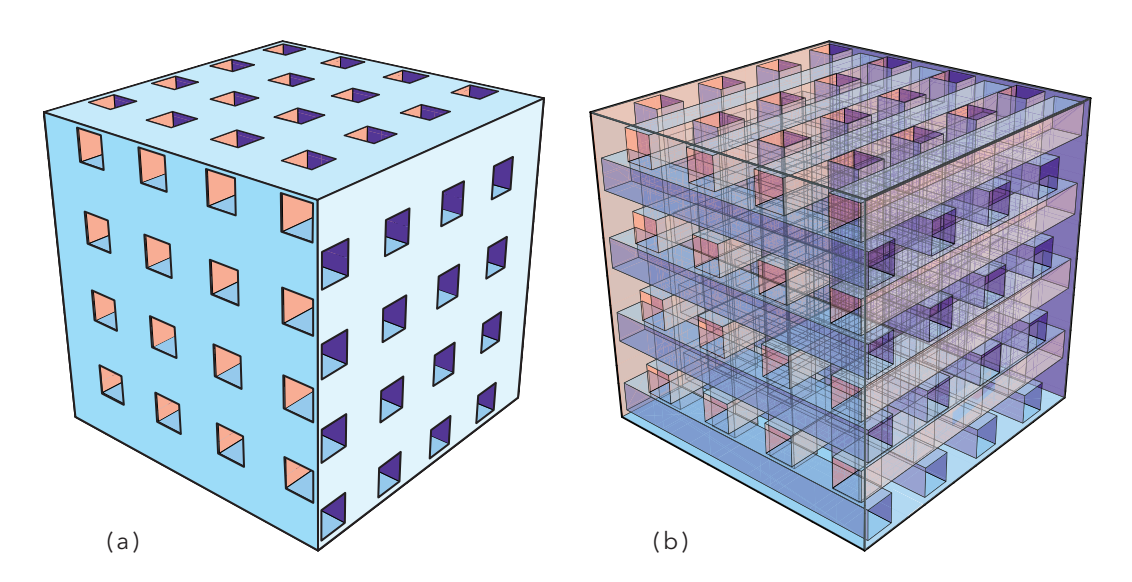


Figure 1.20. (a) The Seidel-Thurston polyhedron with (b) the front three faces removed to reveal the interior.

the front side of the cube, create an $n \times n$ array of 1×1 squares, with a separation of $1 + \varepsilon$ between their rows and columns. Create a tunnel into the cube at each square that does not quite reach all the way through to the back face of the cube, but instead stops ε short of that back face. The result is a deep dent at each square of the front face. Repeat this procedure for the top face and the right face, staggering the squares so their respective dents do not intersect. Now imagine standing deep in the interior, surrounded by dent faces above and below, left and right, fore and aft. From a sufficiently central point, no vertex can be seen!

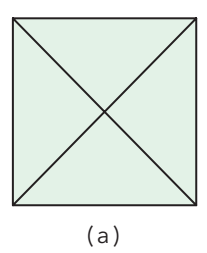
Exercise 1.49. Prove the above claim, which implies that guards at every vertex of the Seidel-Thurston polyhedron do not cover the entire interior. Notice that this implies the polyhedron is not tetrahedralizable.

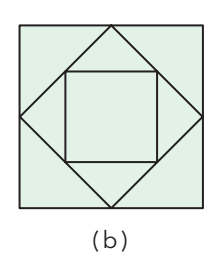
Exercise 1.50. Let n be the number of vertices of the Seidel-Thurston polyhedron. What order of magnitude, as a function of n, is the number of guards needed to cover the entire interior of the polyhedron? (See the Appendix for the Ω notation that captures this notion of "order of magnitude" precisely.)

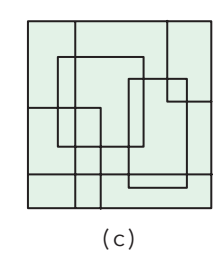
1.5 SCISSORS CONGRUENCE IN 2D

The crucial tool we have employed so far is the triangulation of a polygon *P* by its diagonals. The quantities that have interested us have been combinatorial: the number of edges of *P* and the number of triangles in a triangulation of *P*. Now we loosen the restriction of only cutting *P* along diagonals, permitting arbitrary polygonal cuts. A *dissection* of a polygon *P* cuts *P* into a finite number of smaller polygons. Triangulation can be viewed as an especially constrained form of dissection. The first three diagrams in Figure 1.21 show dissections of a square. Part (d) is not a dissection because one of the partition pieces is not a polygon.

Given a dissection of a polygon P, we can rearrange its smaller polygonal pieces to create a new polygon Q of the same area. Two polygons P and Q are *scissors congruent* if P can be dissected into polygons P_1, \ldots, P_n







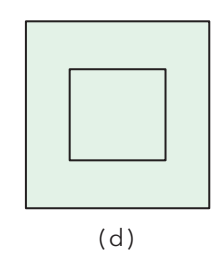


Figure 1.21. Three dissections (a,b,c) of a square, and (d) one that is not a dissection.

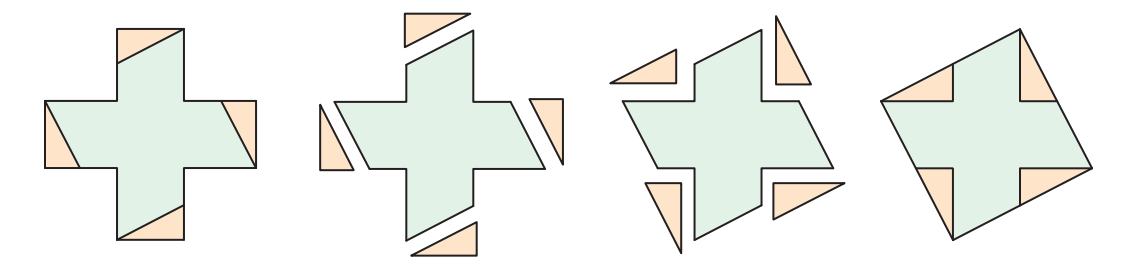


Figure 1.22. The Greek cross is scissors congruent to a square.

which then can be reassembled by rotations and translations to obtain *Q*. Figure 1.22 shows a sequence of steps that dissect the *Greek cross* and rearrange the pieces to form a square, detailed by Henry Dudeney in 1917. However, the idea behind the dissection appears much earlier, in the work of the Persian mathematician and astronomer Mohammad Abu'l-Wafa Al-Buzjani in the 10th century.

The delight of dissections is seeing one familiar shape surprisingly transformed to another, revealing that the second shape is somehow hidden within the first. The novelty and beauty of dissections have attracted puzzle enthusiasts for centuries. Another dissection of the Greek cross, this time rearranged to form an equilateral triangle, discovered by Harry Lindgren in 1961, is shown in Figure 1.23.

Exercise 1.51. Find another dissection of the Greek cross, something quite different from that of Figure 1.22, that rearranges to form a square.

Exercise 1.52. Find a dissection of two Greek crosses whose combined pieces form one square.

Exercise 1.53. Show that any triangle can be dissected using at most three cuts and reassembled to form its mirror image. As usual, rotation and translation of the pieces are permitted, but not reflection.

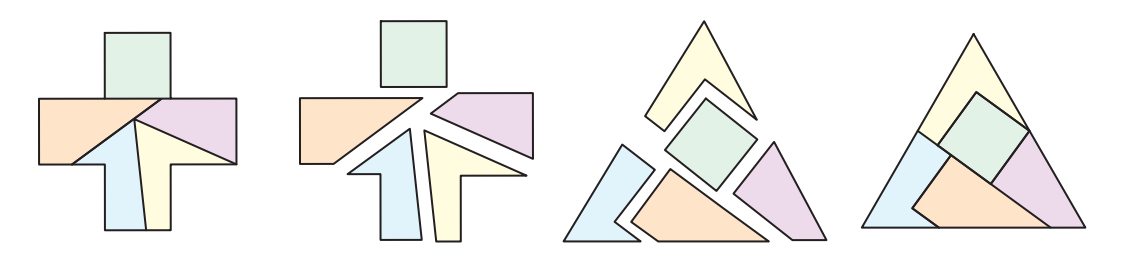


Figure 1.23. Lindgren's dissection of a Greek cross to an equilateral triangle.

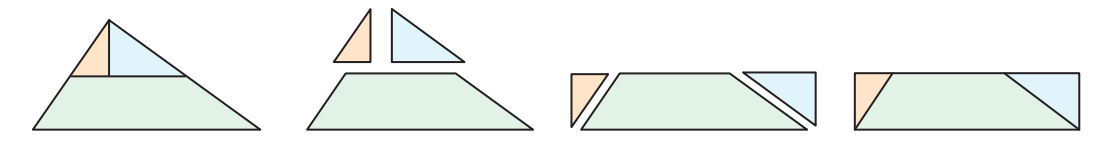


Figure 1.24. Every triangle is scissors congruent with a rectangle.

If we are given two polygons *P* and *Q*, how do we know whether they are scissors congruent? It is obvious that they must have the same area. What other properties or characteristics must they share? Let's look at some special cases.

Lemma 1.54. Every triangle is scissors congruent with some rectangle.

Figure 1.24 illustrates a proof of this lemma. Given any triangle, choose its longest side as its base, of length b. Make a horizontal cut halfway up from the base. From the top vertex, make another cut along the perpendicular from the apex. The pieces can then be rearranged to form a rectangle with half the altitude a of the triangle and the same base b. Note this dissection could serve as a proof that the area of a triangle is ab/2.

Lemma 1.55. Any two rectangles of the same area are scissors congruent.

Proof. Let R_1 be a $(w_1 \times h_1)$ -rectangle and let R_2 be a $(w_2 \times h_2)$ -rectangle, where $w_1 \cdot h_1 = w_2 \cdot h_2$. We may assume that the rectangles are not identical, so that $h_1 \neq h_2$. Without loss of generality, assume $h_2 < h_1 \le w_1 < w_2$.

We know from $w_1 < w_2$ that rectangle R_2 is longer than R_1 . However, for this construction, we do not want it to be *too* long. If $2w_1 < w_2$, then cut R_2 in half (with a vertical cut) and stack the two smaller rectangles on one another. This stacking will reduce the length of R_2 by half but will double its height. However, because $w_1 \cdot h_1 = w_2 \cdot h_2$, the height of the stacked rectangles $2h_2$ will still be less than h_1 . Repeat

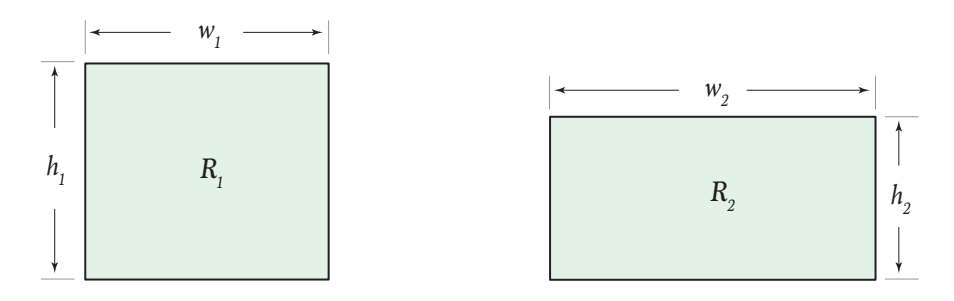


Figure 1.25. Two rectangles satisfying $h_2 < h_1 \le w_1 < w_2 < 2w_1$.

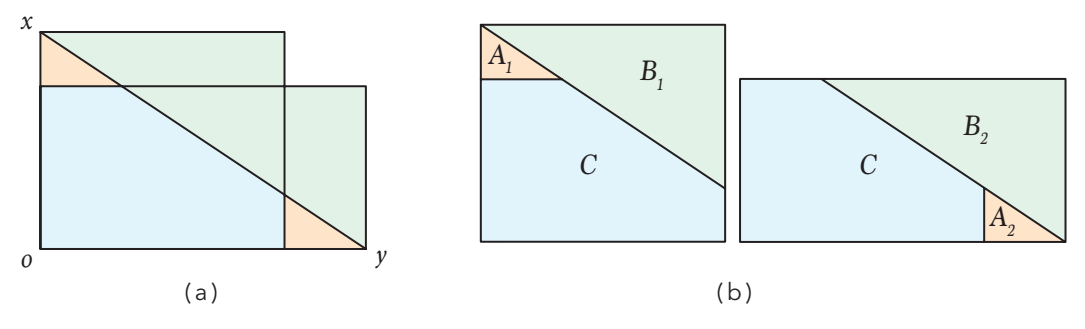


Figure 1.26. Any two rectangles of the same area are scissors congruent.

this process of cutting and stacking until we have two rectangles with $h_2 < h_1 \le w_1 < w_2 < 2w_1$, as shown in Figure 1.25.

After placing R_1 and R_2 so that their lower-left corners coincide and they are flush along their left and base sides, draw the diagonal from x, the top-left corner of R_1 , to y, the bottom-right corner of R_2 . The resulting overlay of lines, as shown in Figure 1.26(a), dissects each rectangle into a small triangle, a large triangle, and a pentagon. We claim that these dissections result in congruent pieces, as depicted in Figure 1.26(b). It is clear the pentagons C are identical. In order to see that the small triangles A_1 and A_2 are congruent, first notice that they are similar to each other as well as similar to the large triangle xoy, as labeled in Figure 1.26(a). Using $w_1 \cdot h_1 = w_2 \cdot h_2$, the equation

$$\frac{h_1 - h_2}{w_2 - w_1} = \frac{h_1}{w_2} \tag{1.2}$$

can be seen to hold by cross multiplying. Because A_1 is similar to xoy, whose altitude/base ratio is h_1/w_2 , and the height of A_1 is $h_1 - h_2$, Equation (1.2) shows that the base of A_1 is $w_2 - w_1$. But since the base length of A_2 is $w_2 - w_1$, it follows that A_1 and A_2 are congruent. A nearly identical argument shows that the large triangles B_1 and B_2 are congruent. The theorem then follows.

Exercise 1.56. Let polygon P_1 be scissors congruent to polygon P_2 , and let polygon P_2 be scissors congruent to polygon P_3 . Show that polygon P_1 is scissors congruent to polygon P_3 . In other words, show that scissors congruence is transitive. We used this transitive property implicitly in the proof of Lemma 1.55 above.

Exercise 1.57. Dissect a 2×1 rectangle into three pieces and rearrange them to form a $\sqrt[3]{4} \times \sqrt[3]{2}$ rectangle.

It is immediate that scissors congruence implies equal area, but the converse is by no means obvious. This fundamental result was proved

independently by William Wallace, Farkas Bolyai, and Paul Gerwien in the early 19th century.

Theorem 1.58 (Wallace–Bolyai–Gerwien). Any two polygons of the same area are scissors congruent.

Proof. Let P and Q be two polygons of the same area α . Using Theorem 1.9, dissect P into n triangles. By Lemma 1.54, each of these triangles is scissors congruent to a rectangle, which yields n rectangles. From Lemma 1.55, these n rectangles are scissors congruent to n other rectangles with base length 1. Stacking these n rectangles on top of one another yields a rectangle R with base length 1 and height α . Using the same method, we see that Q is scissors congruent with R as well. Since P is scissors congruent with R, and R with Q, we know from Exercise 1.56 that P is scissors congruent with Q.

Example 1.59. The Wallace–Bolyai–Gerwien theorem not only proves the existence of a dissection, it gives an algorithm for constructing a dissection. Consider the Greek cross of Figure 1.22, say with total area 5/2. We give a visual sketch of the dissection implied by the proof of the theorem to show scissors congruence with a square of the same area. The first step is a triangulation, as shown in Figure 1.27, converting the cross into 10 triangles, each of area 1/4 and base length 1. Second, each triangle is dissected to a rectangle of width 1 and height 1/4. Finally, these are stacked to form a large rectangle of area 5/2.

Now starting from the square of area 5/2, a triangulation yields two triangles of base length $\sqrt{5}$, as shown in Figure 1.28. Each triangle is then transformed into a $\sqrt{5}/4 \times \sqrt{5}$ rectangle. Each rectangle needs to be transformed into another rectangle of base length 1 (and

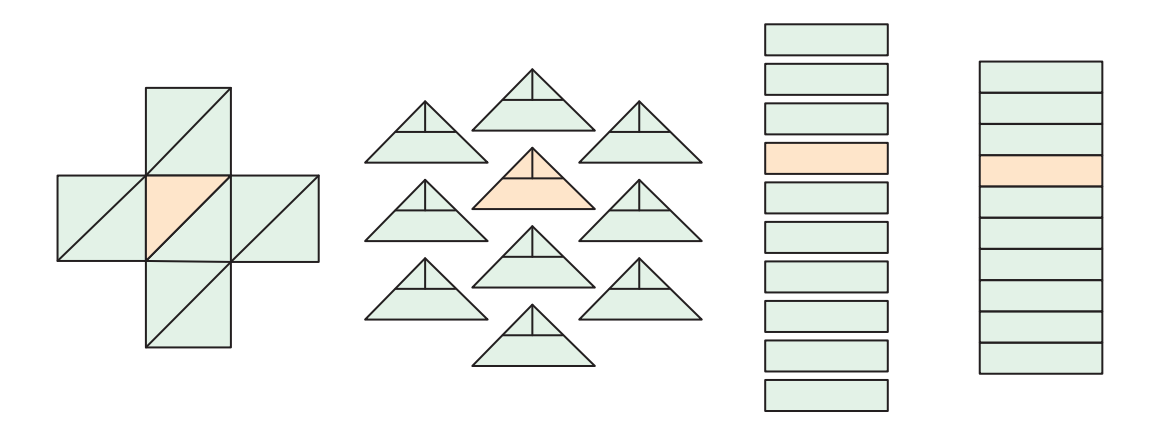


Figure 1.27. Cutting the Greek cross into a rectangle of base length 1 using the Wallace–Bolyai–Gerwien proof. The transformations to the colored triangle are tracked through the stages.

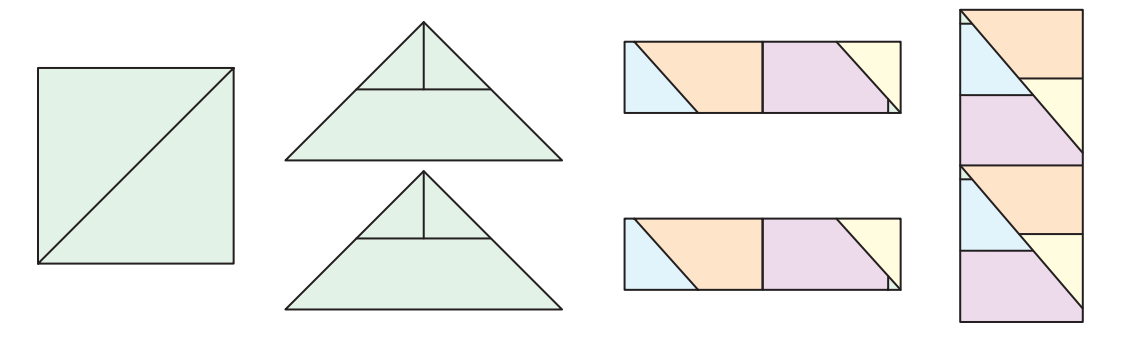


Figure 1.28. Cutting the square into a rectangle of base length 1 using the Wallace–Bolyai–Gerwien proof. The last transformation is color coded to show the fit of the pieces.

height 5/4). Since this rectangle is too long (as described in the proof of Lemma 1.55), it needs to be cut into two pieces and stacked. Then the (stacked) rectangle is cut and rearranged to form two rectangles of base length 1.

Although the Wallace–Bolyai–Gerwien proof is constructive, it is far from optimal in terms of the number of pieces in the dissection. Indeed, we saw in Figure 1.22 that a five-piece dissection suffices to transform the Greek cross to a square.

Exercise 1.60. Following the proof of the Wallace–Bolyai–Gerwien theorem, what is the actual number of polygonal pieces that results from transforming the Greek cross into a square? Assume the total area of the square is 5/2 and use Figures 1.27 and 1.28 for guidance.

Exercise 1.61. Show that a square and a circle are not scissors congruent, even permitting curved cuts.

It is interesting to note that the Wallace–Bolyai–Gerwien theorem is true for polygons not only in the Euclidean plane, but in hyperbolic and elliptic geometry as well. There are also numerous restricted versions of scissors decompositions we may consider, such as the following:

UNSOLVED PROBLEM 6

Fair Partitions

For each positive integer n, is it always possible to partition a given convex polygon into n convex pieces such that each piece has the same area and the same perimeter? This has been established for all prime powers $n = p^k$, where p is a prime and $k \ge 1$ an integer. It remains open for n = 6 and any other n that is not a prime power.

1.6 SCISSORS CONGRUENCE IN 3D

From the discussion above, we see that equal area suffices to guarantee a dissection of one polygon to another. Is this true in higher dimensions? That is, are any two polyhedra of the same volume scissors congruent? Carl Friedrich Gauss, arguably the greatest mathematician since antiquity, asked this question in 1844, about a decade after the Wallace–Bolyai–Gerwien theorem. Figure 1.29 shows an example of a successful dissection, a tetrahedron that is scissors congruent to a triangular prism.

In 1896, French engineer Raoul Bricard claimed to have solved the problem in the negative. Unfortunately, Bricard's proof was flawed, and so, in his famous 1900 address to the International Congress of Mathematicians, the renowned mathematician David Hilbert raised this question again. Within two years, largely based on Bricard's insight, Hilbert's student Max Dehn provided a solution. In particular, Dehn constructed two tetrahedra with congruent bases and the same height which are not scissors congruent. Dehn needed to use powerful algebraic tools to aid his work (known today as tensor products), eventually leading to the larger theory of *Dehn invariants*. Instead of exploring Dehn's difficult proof, we follow Bricard's original proof, now repaired, following ideas of Veniamin Kagan (1903) and David Benko (2007), and relying on the wonderful exposition by Martin Aigner and Günter Ziegler (2010).

Unlike polygons, where angles only appear at the vertices, polyhedra have angles along edges as well. The angle along each edge of a polyhedron, formed by its two adjacent faces, is called the dihedral angle, and forms a key ingredient.

Definition. The *dihedral angle* ϕ at the edge e of a polyhedron shared between two faces f_1 and f_2 is π minus the angle between two unit normal vectors n_1 and n_2 to f_1 and f_2 , respectively. By convention, the

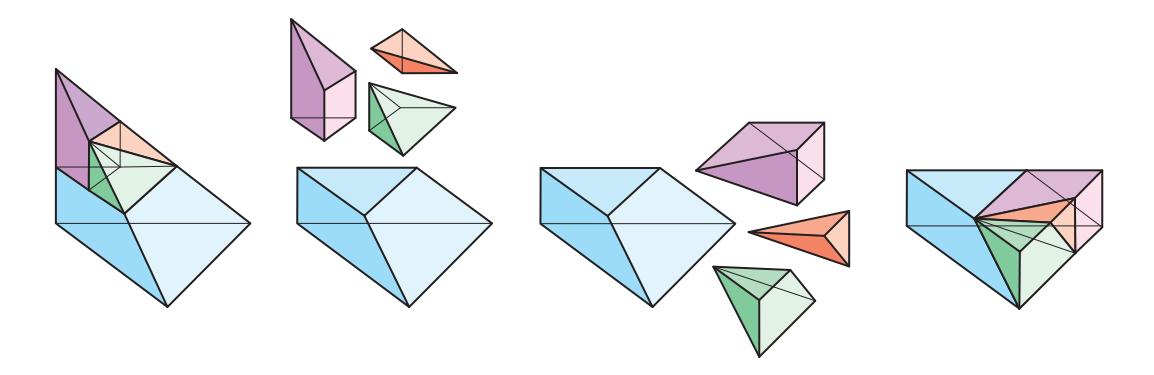


Figure 1.29. Dissection of a tetrahedron to a triangular prism. This tetrahedron is given in Figure 1.30(a), the convex hull of opposing vertical and horizontal edges of a cube. The prism has one-third the height of the tetrahedron.

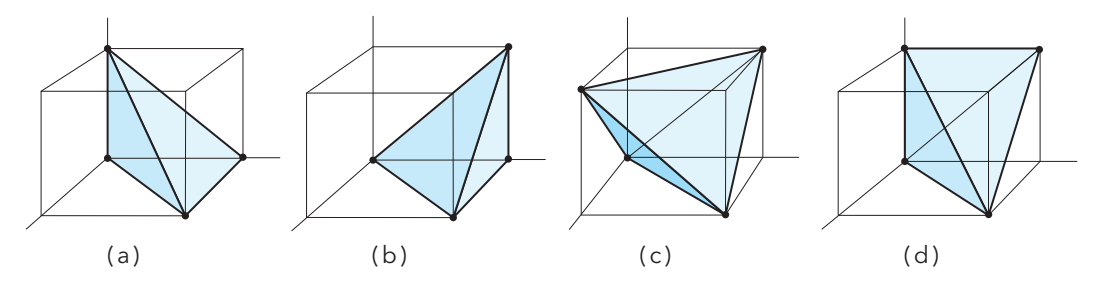


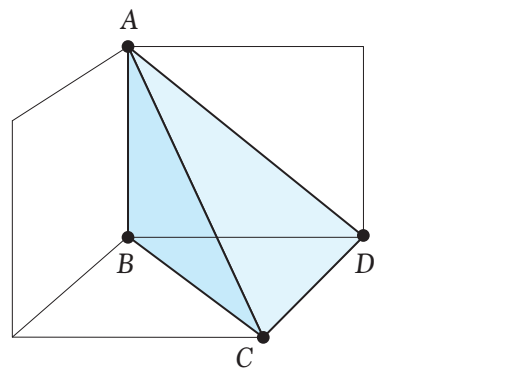
Figure 1.30. Four tetrahedra embedded inside the cube.

normal vectors point to the exterior of the polyhedron, and the dihedral angle at e is the interior angle. Thus $n_1 \cdot n_2 = -\cos \phi$. So at a flat edge between two coplanar faces, n_1 and n_2 coincide, $n_1 \cdot n_2 = 1$ and $\phi = \pi$.

For example, the dihedral angle along each edge of a cube is $\pi/2$. For further examples of dihedral angles, we will use Figure 1.30, which shows four tetrahedra embedded inside the cube.

Example 1.62. The tetrahedron on the left in Figure 1.31 repeats Figure 1.30(a) with labels. The dihedral angle along the edges AD, BC, and BD is $\pi/2$, and the edges AB and CD have dihedral angles of $\pi/4$. To find the dihedral angle along edge AC, we look back at the decomposition of the cube in Figure 1.9 where the cube is tetrahedralized into six polyhedra, each congruent to the polyhedron on the left in Figure 1.31. Thus the dihedral angle along AC is $\pi/3$.

Example 1.63. The tetrahedron on the right in Figure 1.31 repeats Figure 1.30(b). The dihedral angle along the edges *AD*, *BD*, and *CD*



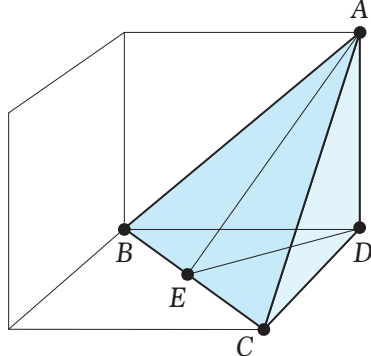


Figure 1.31. Two tetrahedra with congruent bases and the same height. Left tetrahedra dihedral angles: $\pi/2$ (AD, BC, BD), $\pi/4$ (AB, CD), and $\pi/3$ (AC). Right tetrahedra dihedral angles: $\pi/2$ (AD, BD, CD) and $\pi/3$ (AC).

is $\pi/2$, because they are sides of the surrounding cube. Due to symmetry of the polyhedron, the edges AB, AC, and BC have the same dihedral angle. We draw the midpoint E of edge BC in order to calculate the dihedral angle AED along BC. If Figure 1.30(b) is a unit cube (with edge length 1), then the length of DE is $1/\sqrt{2}$. Because the length of AD is 1, the dihedral angle along BC is $\arctan \sqrt{2}$.

Exercise 1.64. Find the dihedral angles of the tetrahedra in Figure 1.30(c) and (d).

★ Exercise 1.65. Find the dihedral angles of the regular dodecahedron, a special polyhedron we explore in Chapter 7. Familiarity with trigonometric identities could help.

When considering scissors congruence, our polyhedra are dissected into numerous smaller polyhedra. We define the *segments* of a dissection to be the 1D subdivisions of all the edges appearing in all the polyhedra. These segments occur in 3D polyhedra as well as in 2D polygons. For example, Figure 1.32 shows two polygons that are scissors congruent, along with their dissections. Notice that *P* and *Q* are each decomposed into three congruent polygonal pieces, with *P* having seven segments and *Q* nine segments.

We can assign variables x_i and y_j to the segments of P and Q, respectively, and obtain a system of linear equations. For the case of Figure 1.32, since the triangles P_i and Q_i are congruent, the lengths of their segments yield nine (nonunique) linear equations:

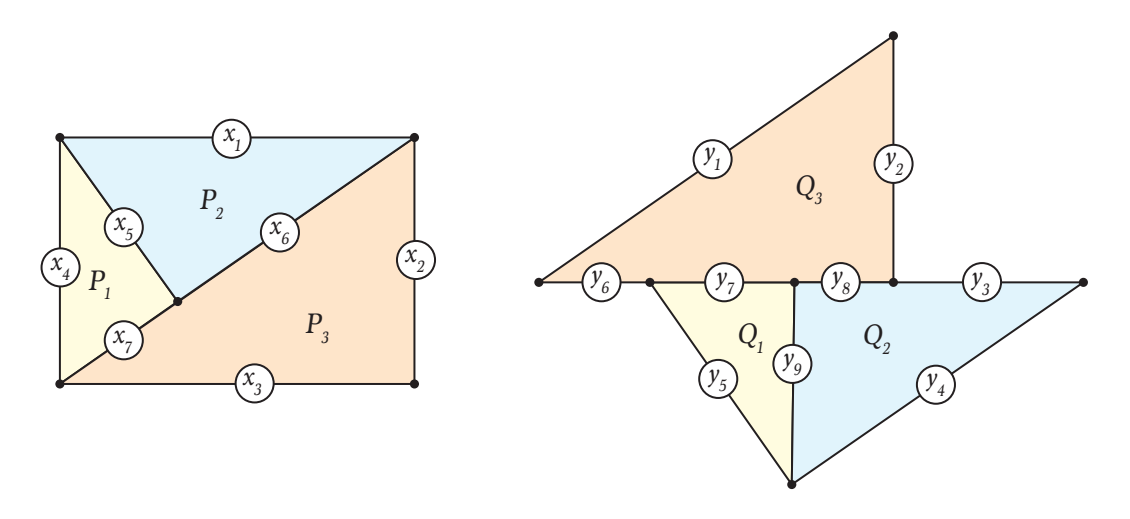


Figure 1.32. Two scissors congruent polygons with their segments labeled.

(continued...)

area

2-coloring, 222, 223

Index

— surface with, 207, 213, 214,

24-, 120-, 600-cell, 204 — differential, 215 218, 219 3-coloring, 18, 255 - surface without, 218, 219 - minimum, 41 3-sum hard, 63 — of polygon, 10, 22, 24, 227 — of Voronoi region, 108, 111 Bricard, Raoul, 28, 32 4-color theorem, 255 — of triangle, 24, 84 4-cube, 243 - vector, 84, 85 Brown, Kevin, 122, 135 Aronov, Boris, 241 Abrahamsen, Mikkel, 257 arrangement carpenter's ruler, 183, 254 Adamaszek, Anna, 257 - combinatorial complexity, 129 cartography, 107 affine transformation, 194 — of hyperplanes, 129 Catalan, Eugène, 11 Aichholzer, Oswin, 97 — of lines, 128–130 Catalan number, 11, 37, 71, 79, Aigner, Martin, 28, 37 - of planes, 132 81, 83, 84, 106 Al-Buzjani, Mohammad — of pseudolines, 134 Cauchy, Augustin-Louis, 170, 221 Abu'l-Wafa, 23 Cauchy's arm lemma, 170–173, art gallery Alexandrov, Alexander D., 241, - minimal number of guards, 256 197, 222, 225 244, 251 — problem, 16, 37, 100, 257 Cauchy's rigidity theorem, 220-222, 224, 226, 244, 251 Alexandrov's gluing theorem, 244, — theorem, 1, 16, 18, 20, 21, 37, 246, 247, 251 255 cavity, topological, 205, 213 algorithm, 4, 41 associahedron, 79-84, 103-106, Čech complex, 168 204, 211 analysis, 44, 46 ceiling function, 17 chain time complexity, 253, 254 and associativity, 82 alpha complex, see α-complex, xiii — graph, 105 — 3D locked, 187 asymptotically optimal, 38, 52, - 3D unit, 187 $\alpha(S)$, see α -complex, xiii α -body, 154, 155, 158 254 — 4D unlocked, 187 α-complex, 158–161 Atiyah-Singer index theorem, 216 - interlocking, 197 Aurenhammer, Franz, 97, 135 - locked, 183, 186, 198; knitting — algorithm, 166 boundary, 161 needles, 197 — filtration, 163 ball, maximal, 143 — planar convex, 170, 171, 173 - inverse, 168 Barvinok, Alexander, 64 — polygonal, 170 — weighted, 168 bellows conjecture, 228, 250 — polygonal, open, 173, 183, 188 α-region, 159, 160, 162 Benko, David, 28 - reflex, 74 chain folding problem, 178, 179 α -shape, 168 Bern, Marshall, 106, 150 AlphaFold, 189, 197 Betti numbers, 213 Chand, Donald, 47 big-Oh notation, vii, 46, 112, 253 Cheong, Otfried, 106, 135 Amenta, Nina, 106, 150 angle big-Omega notation, 22, 46, 254 Chin, Francis, 169 bisector, 138–140, 144 billiards, 36 Chou, Kai-Seng, 198 - deficit, 216 Birkhoff, George, 191 Chow, Bennett, 193, 194 Birkhoff shortening, 191 - dihedral, 28-30, 199, 201, 204, chromatic number, 255 2.2.1 Blum, Harry, 137 Chvátal, Vašek, 18 - face, 200, 202, 216, 226 circle Body(S), see α -body, xiii — interior, 9, 29, 202 Boltyanskii, Vladimir, 37 — osculating, 192 — turn, 9, 172, 173, 218–220, Bolyai, Farkas, 26 - tangent, 154, 192 231, 232, 247 Bonnet, Pierre, 216 — topological, 177 annulus, 180-182 boundary circumcircle antiprism — hull, 41 - empty, 92, 93 — square, 246 — of polygon, 1, 3, 9, 16, 235 — of triangle, 91, 93, 94, 109, 110, - of polyhedron, 199 119-121 any-cut net, 243 Archimedean solids, 203, 204 — shadow, 58, 59, 61–63 clustering, 38

cocircular, 118	— offset, 146, 147; of parabola,	diameter
cocone algorithm, 148	147	— of flip graph, 75, 76, 83, 106
collision detection, 38	— open, 153	— of graph, 75, 83
	— parallel, 146	— of largest circumcircle, 121
combinatorial complexity, 56	_	
combinatorial structure, 97	— reconstruction, 147, 148, 152,	— of point set, 44
configuration	153	Dijkstra, Edsger, 237
— canonical, 183	curve shortening, 197	Dijkstra's algorithm, 237, 238
— flat, 254	— continuous, 192, 193, 195, 198	— continuous, 238, 241
configuration space, 174, 175, 177,	— discrete, 193–195	Dirichlet tessellation, 107
185, 188	cut locus, 136, 137, 235, 236, 241,	disk
— angles, 174–176	242	— bodies, 154
— connected, 183, 185	Cut(P), see cut locus, xiii	— sector, 161
— definition, 173		disk, maximal empty, 136-138,
— of pentagon, 197	D-form, 250	140, 142, 143
. = =		_
— of quadrilateral, 177, 178	Dali, Salvadore, 243	dissection
— topology, 177	— Dali cross, 243	— existence, 26
— of triangulations, 183	De Loera, Jesús, 106	— of Greek cross, 23, 26, 27
connected component, 176	decision-tree model, 46, 51, 254	— hinged, 36
Connelly, Robert, 183, 227	deformation retract, 156, 157	— number of pieces, 27
Conv(S), see convex hull, xiii	degenerate, 64	— of polygon, 22, 23, 28, 37,
convex combination, 39	— polygon, 103	243
convex hull, 38–41	— polyhedron, 203	— of polyhedron, 28
— 3D, 56, 57	— position, 45, 49, 88, 110	— of prism, 28
— 4D, 57, 124	— triangle, 129	— of rectangle, 24, 25
— applications of, 38, 53, 63	Dehn, Max, 28	— segment mass, 32
* *		
— <i>d</i> -dimensional, 57	Dehn invariant, 28	— segment weight, 31
— lower, 51, 122, 123, 126, 131,	Dehn-Hadwiger theorem, 37	— segments, 30
133	Del(S), see Delaunay triangulation,	— of tetrahedron, 28
— of polygon, 51	xiii	divide-and-conquer merge, 53, 55,
— upper, 51, 122, 126	Delaunay, Boris, 89, 119	56, 60–62
convex hull algorithm	Delaunay triangulation, 85, 89, 90,	dodecahedron, 30, 201, 202, 217
		— great, 203, 208
— 2D; divide and conquer, 53, 54,	94–96, 106, 116, 119–124, 131,	
56, 61; gift wrapping, 47–49,	135, 151, 152, 210	dual
59; Graham scan, 49, 50, 58;	— empty circle property, 93	— line, 124
incremental, 41, 42, 44–47, 53,	— fat edge, 88–93	— line, vertical, 124
54, 105; triangle splitting, 105	— flip-graph algorithm, 105	— plane, 124, 125
— 3D; divide and conquer, 61,	— illegal edge, 88	— point, 124
64, 132; gift wrapping, 59;	— legal edge, 88	duality
incremental, 58, 59, 76, 77	— locked edge, 89, 90, 93	— geometric, 124
— higher dimensions, 47, 64	— thin edge, 88–94, 97, 119, 120	Dudeney, Henry, 23
convex position, 65, 71, 79, 80,	Delaunay triangulation algorithm	Dürer, Albrecht, 231
103, 104	— edge flipping, 89, 90, 119	Dürer's problem, 231, 233
convex, strictly, 10	- hull projection, 122, 124	_
convexity, 38, 56, 64, 199, 200	— incremental, 120, 121	Edelsbrunner, Herbert, 106, 122,
Cook, Stephen, 255	Demaine, Erik, 169, 183–185, 198,	135, 169
Cormen, Thomas, 257	251	edge
Corpus Hypercubus, 243	Descartes, René, 217	— contraction, 12
Coxeter, H.S.M., 251	Devadoss, Satyan L., 251	— convex, 199, 226
Cromwell, Peter, 251	Dey, Tamal, 148, 153, 169	— flip, 72, 88
crossing chords, 117, 118	de Berg, Mark, 106, 135	— guard, 20
Crust algorithm, 150, 151, 153,	diagonal	— of polygon, 1
169	— existence, 6	— reflex, 199, 200
— NN-, 153	— external, 10	— of triangulation, 65
crystallography, 107	— noncrossing, 5, 65, 80	elliptic geometry, 27
curvature, 216	— of polygon, 5–7, 9, 11, 16, 53,	envelope
— discrete, 216, 217	65, 80, 83	— lower, 129
— Gaussian, 214, 215, 218	— of polyhedron, 22	— upper, 129
		= =
— geodesic, 218–220	— of triangulation, 72	Eppstein, David, 147, 150, 169
curve	diagonalization, 80, 81, 83-85	ε -sample, 151, 153

Erdős, Paul, 37 Erickson, Jeff, 147, 169 Euclid, 91, 109, 110, 201, 221 Euler, Leonhard, 69, 208 Euler characteristic χ , 212–215, 219, 227 Euler's formula, 56, 69, 70, 77, 102, 112, 156, 197, 205, 208, 210, 211, 213, 214, 220, 221, 251 — proof, 69, 208 exercises, starred, viii existential theory of the reals, 256 $\exists \mathbb{R}$ -complete, 256 exponential time, 254 face angle sum, 202

facility location, 107 filtration — of α-complex, 163, 164, 166 Fisk, Steve, 18, 20 flip graph, 72, 73, 75, 85, 119, 183 — 3D, 78, 79, 105 — animation, 105 — connected, 73, 75, 79, 103, 106,

119 — of convex polygon, 79–81, 83, 85

— and Delaunay triangulation, 90, 94

— diameter, 75

higher dimensions, 79of pseudotriangulation, 103, 104

— shortest path in, 76, 84 floor function, 17, 57

flow

— curve shortening, 192, 193

discrete, 193–196geometric, 192folding

— perimeter halving, 246–248

— refold, 247–249 fortress theorem, 20 Fortune, Steve, 113, 135 Frederickson, Greg, 37

Gage, Michael, 192
Gauss, Carl Friedrich, 28
Gauss–Bonnet theorem, 214–216, 218, 220, 247
— polyhedral, 217–219
— with boundary, 218, 219
Gelfand, Israel, 84
general net, see net, any-cut, 233
general position, 45
— no 2 points on vertical, 53, 55
— no 3 points collinear, 47, 66, 68, 129, 130

— no 4 points cocircular, 88, 89, 93, 94, 110, 113, 118, 119 - no 4 points coplanar, 77, 78 general unfolding, see unfolding, 233 genus, 197, 206, 207, 211-215, 237 geodesic - curvature, 218 - segment, 233 geographic information systems (GIS), 38, 105, 143 Gerwien, Paul, 26 Ghrist, Robert, 169 GIS (geographic information systems), 38, 105, 143 Glickenstein, David, 193, 194 Gluck, Herman, 227 gradient ascent, 90 Graham scan, 58, 63 graph — coloring, 255 — diameter, 75

— coloring, 255
— diameter, 75
— drawing, 189, 198
— dual, 210

— flip, *see* flip graph, xiii — loop, 69

— star, 240 grassfire transformation, 138, 139,

144

Grayson, Matthew, 192 greedy algorithm, 95 Greek cross, 23 Green, Peter, 114 Grünbaum, Branko, 251 guard, 16, 17, 19, 20, 22

— cover, 16–22 — edge, 20 — half-, 100

Haiman, Mark, 81

halfplane

— intersection algorithm, 126, 127

— lower, 126 — upper, 126 Halpern, Dan, 198 Hamilton, Richard, 192 Hanke, Sabine, 76 Harvey, Matthew, 251 heat equation, 191, 197 Hilbert, David, 28, 37 Hoey, Dan, 113 homeomorphism, 205–20

homeomorphism, 205–208 homology, 169, 213 homotopy, 156, 162

— equivalence, 156, 157, 207

type, 157–159
 type of α-complex, 165
 Hong, Se Jun, 53

Hopcroft, John, 178 hyperbolic geometry, 27, 83, 106 hypercube, 15, 204, 243, 244, 250

hyperplane, 131

icosahedron, 201, 202
— truncated, 203, 228, 229
inclusion–exclusion principle, 168
invisible shape, 36

joint

— kinked, 182 — universal, 173 Jonash, Eric, 81 Jordan, Camille, 2 Jordan curve theorem, 2 Joseph, Deborah, 178

Kagan, Veniamin, 28 Kahn, Jeff, 20 Kapala, Sam, 81 Kapranov, Mikhail, 84 Kapur, Sham, 47 Karp, Richard, 255 Kepler, Johannes, 208 kernel, 17, 121, 129 Kettner, Lutz, 64 Klawe, Maria, 20 Klee, Victor, 16 Klein, Rolf, 135 Kleinberg, Jon, 257 Kleitman, Daniel, 20 knitting needles, 170, 185, 186, 197 knot, 206

L'Huilier, Simon, 212 Lakatos, Imre, 251 Latin cross, 228, 229, 248 LaValle, Steven, 198 Lawson, Charles, 73, 106 Lee, Carl, 81

Lee, Carr, 61 Lee, Der-Tsai, 135 Left-of, 48, 63

-4D, 187

- trefoil, 186

— trivial, 187

Krasser, Hannes, 97

Legendre, Adrien-Marie, 208 Leiserson, Charles, 257 Leroy P. Steele Prize, 37 Levin, Leonid, 255

lexicographical ordering, 77, 88

Lindgren, Harry, 23

line

— segment, 1 — of support, 43 linear equations, 30 linear programming (LP), 15

Lipschitz continuity, 154	MWT (minimum weight	perimeter
Lloyd, Errol, 96	triangulation), 94–97	— equipartition, 27
local feature size, 150, 151		— gluing, 246
locus, 136	<i>n</i> -cube, 244	— minimum, 41, 52
lower bounds, 38, 46, 51, 52, 254	<i>n</i> -orthoplex, 244	persistence, 167, 169
LP (linear programming), 15	Näher, Stefan, 64	piecewise linear, 86, 145
	nearest neighbor, 134	pigeonhole principle, 9, 19
machine learning (ML), 38, 168,	nearest-neighbor Crust algorithm,	plane sweep algorithm, 114
189, 197	153	Plato, 201
machining	net, 228, 229, 231, 233, 241	Platonic solids, 34, 199, 201, 202,
— numerically controlled, 143	— any-cut, 243	204, 236, 250
— pocket, 146	— of boxes, 248, 250	Poincaré, Henri, 137, 235
manifold	— common, 248	Poincaré conjecture, 190, 197, 255
— 3- , 177	— of cube, 243	point
— n-, 177	— general, 233, 239, 241, 243	— generic, 240–243
Maxwell-Cremona correspon-	— of hypercube, 243	— round, 192, 194
dence, 250	— of nested prismatoid, 232	polygon, 1
McCammond, Jon, 106	— of truncated icosahedron,	— comb, 17, 18
Med(P), see medial axis, xiii	228	— ear, 9
medial axis, 136-138, 140, 143,	Nicolson, Norman, 227	— exterior, 20
144, 147, 150, 169, 235, 236	NP, nondeterministic polynomial,	— with holes, 6, 10, 20, 83
— 3D, 168	254	— mirror, 36
- algorithm, 140, 142	NP-complete, 8, 16, 96, 178, 254,	— mouth, 10
— of convex polygon, 139–142,	255	— orthogonal, 20, 197
144, 237	NP-hard, 96, 254, 255	orthogonally convex, 63, 189
— digital, 168		— parallel, 189, 197
— parabolic arcs, 142, 143	O(), see big-Oh notation, xiii	— point-in-, 4, 36
— of polyhedron, 138, 139, 145	O'Rourke, Joseph, 37, 64, 169,	— reconstruction, 147–149
— sand, 140	198, 241, 251	— regular, 200
— and Voronoi diagram, 137	octahedron, 201, 202, 204, 227,	- simple, 1, 191, 194, 196, 242
Mehra, Rohan, 227	246, 250	— spherical, 200, 224–226
Michael, T. S., 37	— 4D, 244	— star, 17, 121
midpoint transformation, 190, 191	$\Omega()$, see big-Omega notation,	— star-shaped, 129
Millennium Prize, 255	xiii	polygonization, 63
Miller, Ezra, 244	onion peeling, 63	polyhedral complex, 244
Miltzow, Tillmann, 257	open problems, see unsolved	polyhedron
minimum spanning tree (MST), 96	problems, xiii	— 1-skeleton, 80, 103, 208, 209
minimum weight triangulation	Ottmann, Thomas, 76	— convex, 199, 200, 221, 226, 231;
(MWT), 94–97	output-sensitive algorithm, 48, 57	source unfolding, 239–243; star
Minkowski sum, 168	Overmars, Mark, 106, 135	unfolding, 239, 241, 242
mirror reflection, 36		— definition, 7, 205, 206, 208
Mitchell, Joseph, 238	P, polynomial time, 254	— flattening, 146, 168, 169
miter join, 146, 147	Pak, Igor, 244	— flexible, 227, 250
ML (machine learning), 38, 168,	Papadimitriou, Christos, 239	— medial axis, 138
189, 197	parabola	— megaplex, 37
Monsky's theorem, 36	— convex hull lower bound, 51	— net, see net, xiii
morphing, 105, 184, 189	— directrix, 142	— nonconvex, 200, 211, 220, 221,
— parallel, 190, 197	— focus, 142	227
motion capture, 97	— in medial axis, 142, 143	— orthogonal, 145
motion planning, 107, 188, 198,	— offset curve, 147	— regular, 201, 204
254	— sand, 140, 143	— reshaping, 248
— algorithm, 188	paraboloid, 122–124, 135	— Schönhardt, 8, 21, 36
— complexity, 198	partition	— Seidel–Thurston, 21, 22
— probabilistic roadmap, 188	— of cube, 14	— semiregular, 203, 229, 245
— sofa, 197	— by diagonals, 5	— shaky, 250
motion, expansive, 184	— fair, 27	— Steffen's, 227, 228, 250
Mount, David, 239	— Jordan curve, 3	— straight skeleton, 145
MST (minimum spanning tree),	— of surface by graph, 212, 213	— unfolding; nonoverlap, 228,
96 Mulzor Wolfgang 96	— into tetrahedra, 7, 15	233, 242; overlap, 231
Mulzer, Wolfgang, 96	pattern recognition, 38, 107	— uniform, 203

polytope polygon, 17, 121 Schuierer, Sven, 76 -4D, 204 scissors congruent — of vertex, 74, 75 associahedron, 81, 82, 103 - 2D, 22-27 Stasheff, James, 81 - 3D, 28, 34, 37 Steffen, Klaus, 227 — convex, 243, 244 — cross, 204 — transitive, 25 Stein, Cliff, 257 - regular, 81, 204, 250, 251 Sedgewick, Robert, 257 Steiner, Jakob, 98 secondary, 84, 106 segment, line, 1 Steiner point, 98–100 Preparata, Franco, 52, 53, 64 Seidel, Raimund, 8, 21, 64, 122, Steinitz, Ernst, 170, 171 primal plane, 124, 125 straight skeleton, 143-146, 169 priority queue, 142 set partition problem, 178, 254, — of polyhedron, 145, 146 prism 255 Streinu, Ileana, 103 Shamos, Michael, 52, 64, 113 supporting line, 43 — antiprism, 246 — rectangular, 35 shape surface — triangular, 78 — α -complex, 158 — connected, 205 prismatoid, 232 biological, 137 orientable, 211, 213 nested, 232 - filtration, 167 - reconstruction, 148, 153, 168, prismoid, 233 — medial axis, 136 169 proof sketch, viii — of point set, 136, 154 Sydler, Jean-Pierre, 34 protein - of polygon, 136 Sydler's theorem, 36 — folding, 170, 188, 197 — topological, 156 - structure, 188 Sharir, Micha, 71, 198, 239 Tamassia, Roberto, 198 pseudoline, 134 Sheffer, Adam, 71 tangent pseudotriangle, 100, 101 — circle, 154, 192 Shewchuck, Jonathan, 105, pseudotriangulation, 101, 102, 106 — line, 43, 44, 47, 53–56, 61 104, 105, 184 shortest path - plane, 61, 122, 131, 218 - in flip graph, 76, 84 Tardos, Éva, 257 minimal, 102 pointed, 101–104 in graph, 237 Tarjan, Robert, 83, 106 — in polygon, 11, 235 terrain, 86, 87, 122 quench point, 136, 138 — on polyhedron, 233–236, 239, — reconstruction, 86, 87 242; algorithm, 237, 238 tesseract, see 4-cube, xiii, 15 Rambau, Jörg, 106 Sibson, Robin, 114 tetrahedralization, 1, 7, 14, 15, 21, reachability region, 180, 182 sign alternation, 222, 225, 226 36, 76, 77, 79, 105, 106 recursion vs. induction, 53 simplex — of cube, 7, 14, 15 reflex, 11 **—** 4-, 204 — Delaunay, 124 reflex chain, 71, 100 -n-, 15, 204 — impossible, 8, 21, 22 regular subdivision, 106 simply connected, 1 — number of tetrahedra, 77, 78 rendezvous problem, 195 Skel(P), see straight skeleton, — space of, 78 Riemann-Roch theorem, 216 tetrahedron, 250 xiii Sleator, Daniel, 83, 106 Thales' theorem, 91, 93 rigid, infinitesimally, 227 Rivest, Ron, 257 Snoeyink, Jack, 169 Thiessen polygons, 107 Thurston, William P., 21, 83, 106, robot arm, 173, 174, 178, 188, software 254 — ArcGIS, 105 251 — hand, 173 - CGAL, 63, 64 tiling, 250 — motion, 170 — LEDA, 64 TIN (triangulated irregular — reachability, 179–182, 198 - Mathematica, 63 network), 105 — shoulder, 173 — Matlab, 63, 105 topological data analysis, 167 robust computation, 64 — polymake, 63 topology, 176 Rote, Günter, 96, 103, 183 space complexity, 253 torus, 175, 176, 206, 229 Ruppert, Jim, 8 spanning tree, 96, 208, 209, 237, — linked, 167 242, 243 — n-dimensional, 177 Saalfeld, Alan, 98 — minimum (MST), 96, 97 Toussaint, Godfried, 20 Sabitov, Idzhad, 227 special orthogonal group SO(3), traveling salesman problem (TSP), Salzman, Oren, 198 177 2.56 Santos, Francisco, 79, 103, sphere tree 106 **—** 3-, 177 interdigitating, 210 Schirra, Stefan, 64 - polyhedral, 206, 210, 218 triangle Schläfli, Ludwig, 203 — topological, 176 - minimum area, 129 Schläfli symbol, 203, 205 Stanley, Richard, 37 - minimum area algorithm, Schlegel diagram, 204, 209 130 star

— graph, 240

Schreiber, Yevgeny, 239

- skinny, 87, 94

triangulated irregular network von Staudt, Karl, 208 Compatible Triangulations in (TIN), 105 Simple Polygons (#14), 100 Vor(S), see Voronoi diagram, xiii triangulation — Counting Triangulations (#2), 14 Voronoi, Georgy, 107, 119 — 3-coloring, 18 — Discrete Flow (#22), 195 Voronoi diagram, 107, 108, 124, — canonical, 183 — Dürer's Problem (#23), 231 131, 135, 136, 244 - compatible, 97, 98, 100, 105 — Edge Guards (#5), 20 — and arrangements, 135 — Fair Partitions (#6), 27 — combinatorial complexity, 112, — of convex polygon, 11, 13 — counting algorithm, 72 — Five-Piece Puzzle (#7), 35 113, 121 - dual, 82, 118, 119, 131 - Flip Graph in 3D (#10), 79 - and cut locus, 240, 241 — existence, 5–7 Minimum Triangulations of — disconnected, 112 — fatness, 88–90, 119 Cubes (#3), 15 — dual, 116–119, 131, 210 - greedy, 96 Minimum Weight Triangulation - dynamic, 134 — inducing, 15 (#12), 97— edge, 108, 111, 133 minimum weight (MWT), Open Curve Reconstruction — farthest point, 132–134 94-97 (#18), 153- game, 134 — n-dimensional, 15 -- P = NP (#28), 255 - geometry, 107 — number of, 10, 13, 14, 71 Pointed Pseudotriangulations — kth-order, 134 - number of triangles, 9, 10, 69, (#15), 104of lines in 3D, 121 71 - Shortest Path in Flip Graph - and medial axis, 137 - Pitteway, 119 (#11), 84— in nature, 134 — of point set, 65 Spaces for Simple Polygons — one-dimensional, 116 — of polygon, 1, 5 (#19), 185— of polygon, 146 - Straight Skeleton (#17), 146 — of polygon with holes, 6 - region, 107-109, 113, 116, — space of, 73, 183 Tetrahedralizable Polyhedra 133 - unique, 10, 13, 14, 119 (#1), 8- sand, 134 triangulation algorithm Triangulation Counting — uniqueness, 119 — incremental, 68, 69, 74, 183 Algorithm (#9), 71 — from upper envelope, 131 — triangle splitting, 66–69 Unfold and Refold (#27), 249 — vertex, 108–111, 133, 151 Trossen Robotics, 173 Unfolding Prismatoids (#24), Voronoi diagram algorithm, 112, TSP (traveling salesman problem), 256 Visibility Graphs (#4), 18 — divide and conquer, 133 Voronoi Diagram of Lines in 3D - Fortune's plane sweep, 114, Uehara, Ryuhei, 250 (#16), 121133, 135 unfolding upper bounds, 46, 253 incremental, 114, 115, 121 - any-cut, 241 Urrutia, Jorge, 37 Voronoi map, 134 - edge, 229, 231-233, 244 - refold, 247-249 van Kreveld, Marc, 106, 135 Wallace, William, 26 Wallace-Bolyai-Gerwien theorem, - ridge, 244 vertex 26, 27, 248 - source, 239, 241-244 — convex, 10 - star, 239-241, 243, 244 — flat, 1, 10, 45, 202, 203 Wang, Cao An, 169 uniform distribution, 47 — of polygon, 1 Whitesides, Sue, 178 unsolved problems, viii — reflex, 10, 11, 13, 14, 17, 142, width — 3D Graham Scan (#8), 58 144, 146 — of point set, 63 - 3D Locked Chains (#21), 187 visibility, 16, 20, 38, 43, 46, 59, wrapping, 250 - 3D Unit Chains (#20), 187 68, 242 Alexandrov Folding (#26), 247 — of face, 59 Zaremba, Stanislaw, 171 Zelevinsky, Andrei, 84 — Any-Cut Nets (#25), 243 — graph, 18 Compatible Triangulations -k-, 36 Zhu, Xi-Ping, 198 (#13), 98— x-ray, 36 Ziegler, Günter, 28, 37